8-Bicycloalkyl-CPFPX Derivatives as Potent and Selective Tools for in vivo Imaging of the A_1 Adenosine Receptor

Humpert S.[a], Schneider D.[a], Bier D.[a], Schulze A.[a], Neumaier F.[a,b], Neumaier B.[a,b,c*], Holschbach M.[a]

[a] Forschungszentrum Jülich GmbH, Institute of Neurosciences and Medicine, Nuclear Chemistry (INM-5), Wilhelm-Johnen-Str., 52428 Jülich, Germany

[b] Institute of Radiochemistry and Experimental Molecular Imaging, Faculty of Medicine and University Hospital Cologne, University of Cologne, Kerpener Str. 62, 50937 Cologne, Germany

[c] Max Planck Institute for Metabolism Research, Gleueler Straße 50, 50931, Cologne, Germany.

* Corresponding author: b.neumaier@fz-juelich.de

Abstract

Imaging of the A_1 adenosine receptor (A_1R) by positron emission tomography (PET) with 8-cyclopentyl-3-(3-[^{18}F]fluoropropyl)-1-propyl-xanthine ([^{18}F]CPFPX) has been widely used in preclinical and clinical studies. However, this radioligand suffers from rapid peripheral metabolism and subsequent accumulation of radiometabolites in the vascular compartment. In the present work, we prepared four derivatives of CPFPX by replacement of the cyclopentyl group with norbornane moieties. These derivatives were evaluated by competition binding studies, microsomal stability assays and LC-MS analysis of microsomal metabolites. In addition, the ^{18}F-labeled isotopologue of 8-(1-norbornyl)-3-(3-fluoropropyl)-1-propylxanthine (1-NBX) as the most promising candidate was prepared by radiofluorination of the corresponding tosylate precursor and the resulting radioligand ([^{18}F]1-NBX) was evaluated by permeability assays with Caco-2 cells and in vitro autoradiography in rat brain slices. Our results demonstrate that 1-NBX exhibits significantly improved A_1R affinity and selectivity when compared to CPFPX and that it does not give rise to lipophilic metabolites expected to cross the blood-brain-barrier in microsomal assays. Furthermore, [^{18}F]1-NBX showed a high passive permeability (P_c = 6.9±2.9 × 10^{-5} cm/s) and in vitro autoradiography with this radioligand resulted in a distribution pattern matching A_1R expression in the brain. Moreover, a low degree of non-specific binding (5%) was observed. Taken together, these findings identify [^{18}F]1-NBX as a promising candidate for further preclinical evaluation as potential PET tracer for A_1R imaging.

Keywords: Positron emission tomography, adenosine A_1 receptor ligand, fluorine-18 labelling, ligand design, autoradiography

Abbreviations: 1-NBX, 8-(1-norbornyl)-3-(3-fluoropropyl)-1-propylxanthine; 1-NBXOF, 8-(1-norbornyl)-3-(2-(2-fluoroethoxy)ethyl)-1-propylxanthine; 2-NBX, 8-(2-norbornyl)-3-(3-fluoropropyl)-1-propylxanthine; 7-NBX, 8-(7-norbornyl)-3-(3-fluoropropyl)-1-propylxanthine; A_1R, A_1 adenosine receptor; $A_{2A}R$, A_{2A} adenosine receptor; $A_{2B}R$, A_{2B} adenosine receptor; A_3R, A_3 adenosine receptor; BBB, blood-brain barrier; clogP, calculated partition coefficient; CNS, central nervous system; CPFPX, 8-cyclopentyl-3-(3-fluoropropyl)-1-propyl-xanthine; DMB; 2,4-dimethoxybenzyl; DPCPX; 8-cyclopentyl-1,3-dipropylxanthine; FBS, fetal bovine serum; FC, flash chromatography; k', capacity factor; K_d, dissociation constant; K_i, inhibition constant; LiDDB, lithium 4,4'di-*tert*-butylbiphenylide; logP; experimental partition coefficient; Ms, methanesulfonyl; NAX, noradamantylxanthine; NBX, norbornyl-substituted xanthine; PET, positron emission tomography; Pom, pivaloyloxymethyl; Pom-Cl, pivaloyloxymethyl chloride; R_t, retention time; (*S*)-ENX, 2-(5,6-epoxynorbornyl)xanthine; TEER, transepithelial electrical resistance; Ts, *p*-toluenesulfonyl.

1. Introduction

Adenosine is an ubiquitous, predominantly inhibitory neuromodulator in the central nervous system (CNS)[1] involved in numerous physiological (e.g., regulation of sleep[2] and synaptic plasticity[3]) and pathological (e.g., Alzheimer's disease[4] and Parkinson's disease[5]) processes. Extracellular adenosine can exert its effects on neuronal transmission by interaction with four different adenosine receptors, which comprise the high-affinity A_1R (EC_{50}: 70-100 nM) and $A_{2A}R$ (EC_{50}: 150-310 nM) subtypes, and the lower affinity $A_{2B}R$ (EC_{50}: 5-15 µM) and A_3R (EC_{50}: 0.3-6.5 µM) subtypes. In the brain, A_1R is the most abundant member and widely distributed in the cortex, hippocampus, and cerebellum[6]. Owing to its physiological relevance and heterogenous brain distribution that may be altered by normal aging, sleep deprivation and under pathological conditions, non-invasive imaging of the A_1R with selective PET radioligands has become an important tool for preclinical and clinical research[7].

The current gold standard for in vivo PET imaging of A_1R is 8-cyclopentyl-3-(3-[^{18}F]fluoropropyl)-1-propyl-xanthine ([^{18}F]CPFPX)[8], an ^{18}F-labeled analog of the prototypical A_1R antagonist 8-cyclopentyl-1,3-dipropylxanthine (DPCPX) (Fig 1A). This radioligand is resistant to metabolic enzymes present in the brain and has been successfully used for many preclinical and clinical studies[9]. However, it suffers from rapid hepatic clearance (in vitro $t_{1/2}$ = 14 min in liver microsomes), so that the fraction of intact radioligand in plasma quickly declines (terminal in vivo $t_{1/2}$ = 15 min in rats)[10]. Functionalization occurs predominantly at the methine group (tertiary carbon) of the cyclopentyl ring[11] and results in polar radiometabolites that are unlikely to cross the blood-brain barrier (BBB). Nevertheless, rapid peripheral metabolism could reduce brain delivery of intact tracer, since passive diffusion across the BBB is driven by the concentration gradient. In addition, the bifunctionalized enone species (enone-type molecule) formed as main metabolite in humans is only slowly excreted and accumulates in the vascular compartment, reducing attainable target-to-background ratios due to enhanced background activity[12]. As such, there is still a need for radioligands with improved imaging properties that enable, e.g., reliable quantification of A_1R in brain regions with low receptor abundance.

Initially, our efforts to develop such radioligands focused on metabolically stabilized CPFPX derivatives. However, a recent work by Schneider et al.[13] demonstrated that slower plasma clearance does not necessarily improve the suitability of xanthine-based A_1R radioligands for PET imaging, most likely because fast BBB penetration of these compounds results in extensive brain extraction within the first few minutes after administration (i.e. before peripheral metabolism can significantly reduce the fraction of tracer available for brain entry). In contrast, high receptor affinity proved to be a key factor for the cerebral pharmacokinetics and in vivo performance of radiolabeled xanthines, which prompted us to focus on the synthesis of A_1R ligands with improved affinity.

The effects of varying the alkyl substituents at the 1- and 3-positions and of substituents at the 8-position of the xanthine moiety on the activity and selectivity of xanthines for adenosine receptors are

well known. In particular, propyl groups at the 1- and 3-positions have been shown to confer higher potency than smaller (methyl, ethyl) or larger (butyl, isoamyl) residues[14]. On the other hand, introduction of certain aryl or cycloalkyl substituents at C-8 in 1,3-dimethylxanthine (theophylline) and 1,3-dipropylxanthine markedly increased affinity at the A_1R[15].

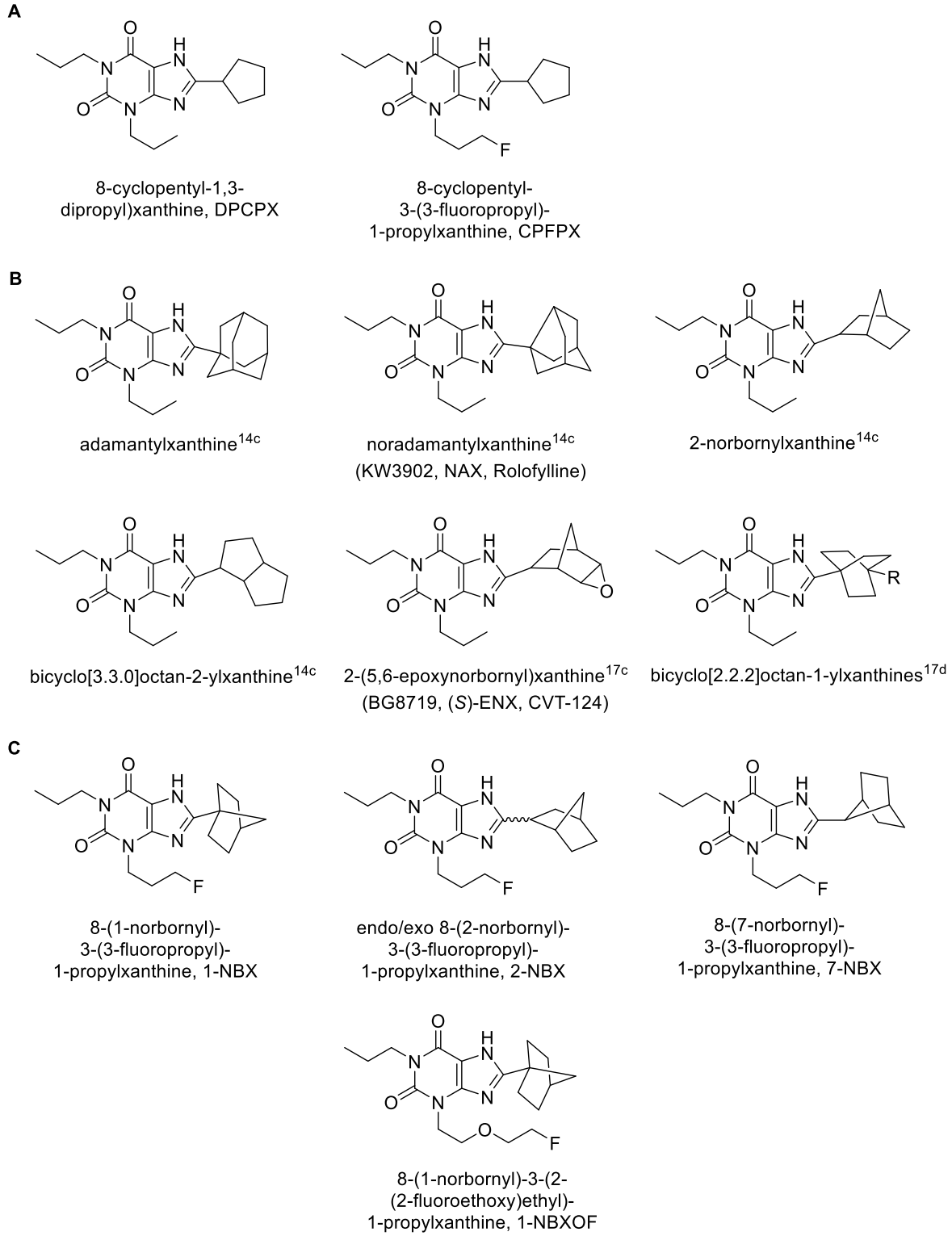

Figure 1: Structure of known A_1R antagonists consisting of a 1,3-dipropylxanthine backbone with a 8-cyclopentyl residue (A) or other bulky substituents at the 8-position (B) as well as of the new norbornyl analogs described in the present work (C).

Among 8-substituted congeners, DPCPX (Fig 1A) proved to possess particularly high activity and selectivity[16], so that its tritiated isotopologue [^{3}H]DPCPX has remained the gold standard A_1R antagonist for in vitro studies. In addition, there are many other examples of potent A_1R antagonists consisting of a 1,3-dipropylxanthine backbone with a bulky lipophilic substituent at the 8-position[17] (Fig. 1B).

In search for A_1R radioligands with improved target affinity, we therefore decided to replace the 8-cyclopentyl residue of the xanthine backbone in CPFPX with sterically more demanding, rigid bicycloalkyl residues[14c, 18]. Bicycloalkyl substituents selected for the present work comprised three isomeric bicyclo[2.2.1]heptane (norbornane) moieties, namely 1-, 2- and 7-norbornyl residues (Fig. 1C). Additionally, a 1-norbornyl derivative with an alternative *N*-3 residue was included to evaluate how replacement of the 3-fluoropropyl group in this position by a larger substituent with an ether function affects the binding properties.

2. Results and Discussion

2.1. Chemistry

The required starting carboxylic acid bicyclo[2.2.1]heptane-2-carboxylic acid (2-norbornanecarboxylic acid) (**1**) was commercially available, while bicyclo[2.2.1]heptane-1-carboxylic acid (1-norbornanecarboxylic acid) (**3**) and bicyclo[2.2.1]heptane-7-carboxylic acid (7-norbornanecarboxylic acid) (**5**) were prepared by the following known methods: The synthesis of 1-norbornanecarboxylic acid **3** (Scheme 1a) started from the isomeric 2-norbornanecarboxylic acid (**1**), which was brominated under Hell-Volhard-Zelinsky conditions accompanied by a Wagner-Meerwein rearrangement[19]. Thus, reaction of **1** with elemental bromine and a catalytic amount of phosphorous trichloride furnished the intermediate 2-bromonorbornane-1-carboxylic acid (**2**) in 78% yield[20]. Reductive debromination of **2** with zinc powder and acetic acid under reflux provided the desired 1-norbornanecarboxylic acid **3** in a yield of 81%[21].

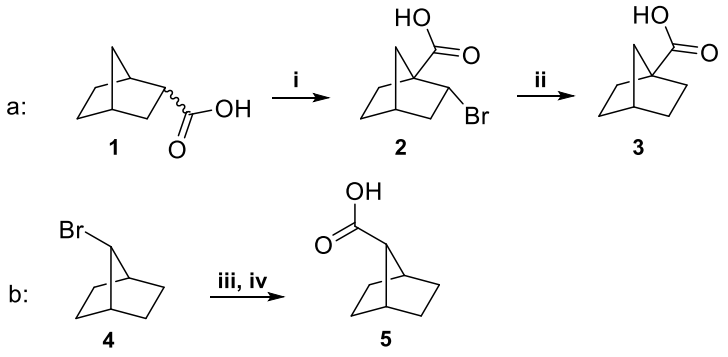

Scheme 1: Synthesis of a: 1-norbornanecarboxylic acid (**3**) and b: 7-norbornanecarboxylic acid (**5**). Conditions: **i**: Br_2, PCl_3, reflux; **ii**: zinc powder / acetic acid, reflux; **iii**: lithium 4,4'-di-*tert*-butylbiphenylide; **iv**: CO_2.

7-Norbornanecarboxylic acid **5** (Scheme 1b) was prepared from 7-bromonorbornane (**4**) following the procedure described by Stapersma and Klumpp[22], which entails a halogen–lithium exchange reaction and subsequent carboxylation of the lithiated norbornane intermediate with carbon dioxide. Accordingly, reaction of alkyl bromide **4** with lithium 4,4'di-*tert*-butylbiphenylide (LiDDB)[23] followed by treatment with solid carbon dioxide provided 7-norbornanecarboxylic acid **5** in near quantitative yield. The target norbornyl-substituted xanthines (NBX) **11a**-**c** and radiofluorination precursor **13a** were prepared using multistep syntheses based on a modified Traube protocol (Scheme 2)[24]. Thus, the xanthine intermediates **7a-c** were obtained in two steps by condensing 5,6-diamino-1-(2,4-dimethoxybenzyl)-3-propyluracil (**6**) with the acids **1**, **3** or **5** by the mixed anhydride method with isobutyl chloroformate and *N*-methylmorpholine as a base, which was directly followed by alkaline ring closure of the resulting carboxamides with aqueous sodium hydroxide in 1,4-dioxane. Subsequent protection of *N*-7 by alkylation with pivaloyloxymethyl chloride (Pom-Cl) gave **8a-c**, which underwent clean debenzylation upon treatment with methanesulfonic acid and triethylsilane to form **9a-c**. Subsequent alkylation of *N*-3 with 3-fluoropropyl mesylate gave **10a-c**, which were subjected to alkaline hydrolysis with aqueous sodium hydroxide in methanol to remove the Pom group and yield the respective 3-(3-fluoropropyl)-1-propylxanthines (**11a-c**).

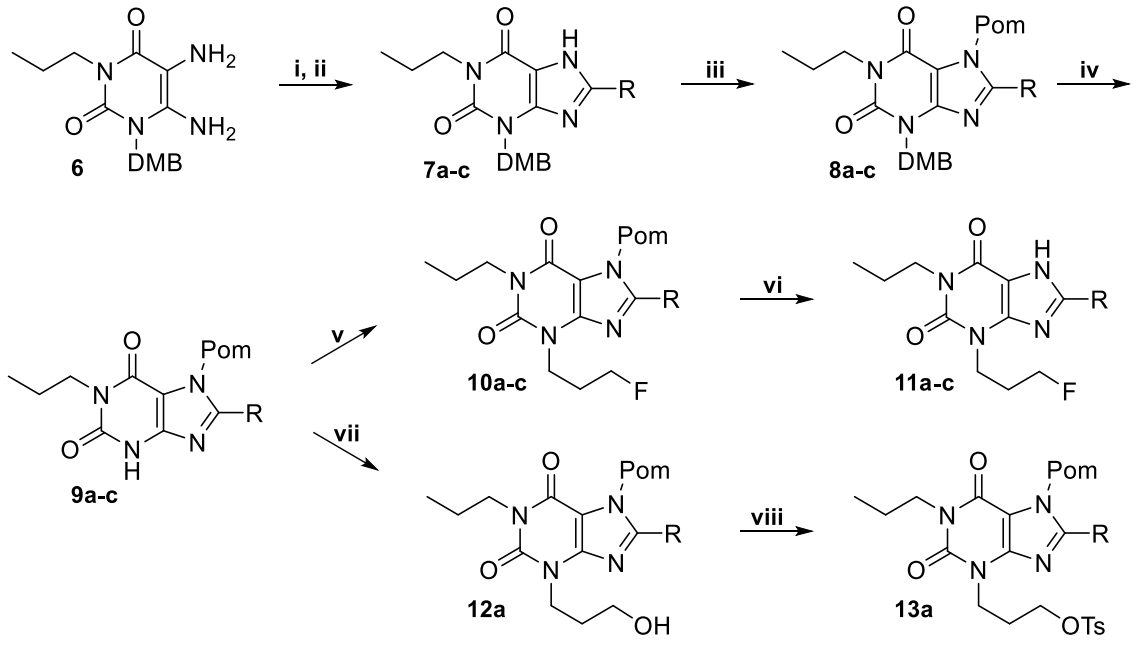

R = 1-norbornyl (**a**), 7-norbornyl (**b**) or endo/exo 2-norbornyl (**c**)

Scheme 2: Synthesis of target xanthines **11a**-**c** and radiolabeling precursor **13a**. Conditions: **i**: RCO_2H, isobutyl chloroformate / *N*-methylmorpholine; **ii**: 2 N NaOH, dioxane, reflux; **iii**: Pom-Cl, K_2CO_3, DMF; **iv**: methanesulfonic acid / Et_3SiH / DCM; **v**: 3-fluoropropyl mesylate, K_2CO_3, DMF; **vi**: NaOH / methanol; **vii**: 3-bromopropanol, K_2CO_3, DMF; **viii**: *p*-toluenesulfonyl chloride (TsCl), 1,6-bis(dimethylamino)hexane. Abbreviations: DMB, 2,4-dimethoxybenzyl; Pom, pivaloyloxymethyl; Ts, *p*-toluenesulfonyl.

Radiofluorination precursor **13a** was obtained by *N*-3 alkylation of **9a** with 3-bromo-1-propanol, followed by esterification of the resulting alcohol **12a** with toluenesulfonyl chloride and 1,6-bis(dimethylamino)hexane[25].

Compound **17** (Scheme 3) was prepared by *N*-3 alkylation of **9a** with 2-(2-chloroethoxy)ethanol to furnish alcohol **14**. The hydroxyl function of **14** was activated towards nucleophilic fluorination by transformation into a methanesulfonate ester. The mesylate **15** thus obtained was then treated with cesium fluoride in *tert*-butanol[26] followed by alkaline Pom-deprotection of the fluorinated intermediate **16** to provide the target xanthine **17**.

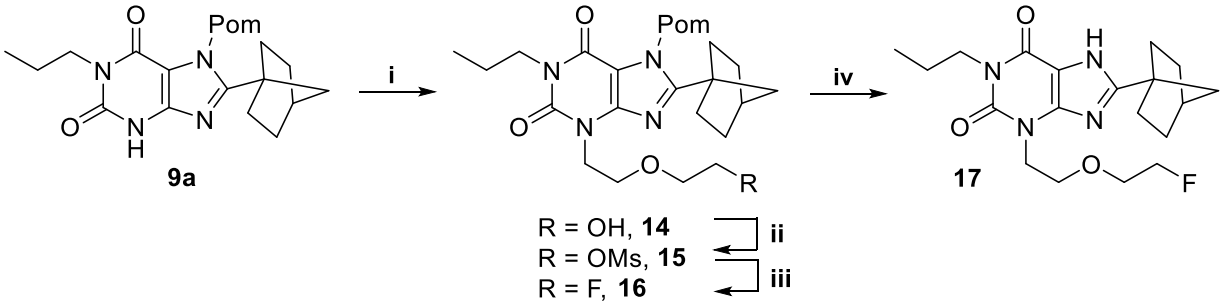

Scheme 3: Synthesis of xanthine **17**. Conditions: **i**: 2-(2-chloroethoxy)ethanol, K_2CO_3, DMF; **ii**: methanesulfonyl chloride, triethylamine; **iii**: CsF, *tert*-butanol; **iv**: NaOH / methanol. Abbreviations: Pom, pivaloyloxymethyl; Ms, methanesulfonyl.

Radiotracer [^{18}F]1-NBX ([^{18}F]**11a**) was prepared from the Pom-protected tosylate precursor **13a** using the same conditions as previously described for the preparation of [^{18}F]CPFPX[8] (Scheme 4). Briefly, after azeotropic drying of [^{18}F]fluoride, the precursor was labeled at 85 °C in DMSO using the Kryptofix 2.2.2/K_2CO_3 system[27], followed by deprotection with aqueous sodium hydroxide.

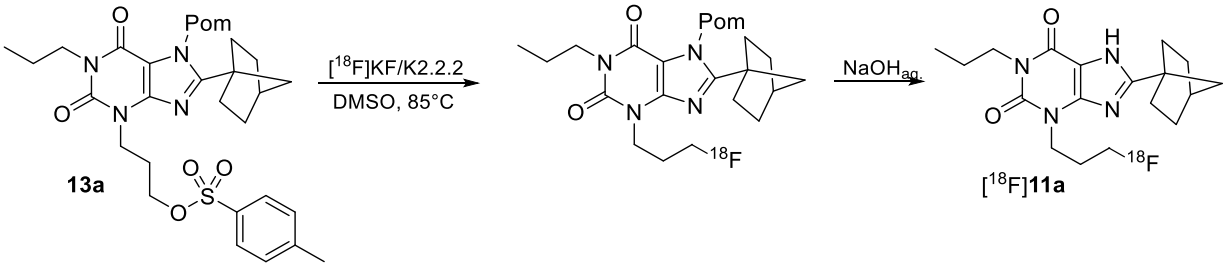

Scheme 4: Preparation of [^{18}F]1-NBX ([^{18}F]**11a**) by nucleophilic radiofluorination of precursor **13a**.

Purification by semipreparative HPLC furnished the radiotracer in radiochemical yields of 40 ± 10%, a radiochemical purity of >99%, a molar activity of 50-200 GBq/µmol (n=3, 200-840 MBq product, 0.2-1.1 µg/mL carrier) and high chemical purity (0.5-1.1 µg/mL chemical impurities). The identity of the radiolabeled compound was confirmed via HPLC by comparing the retention time with that of the non-radioactive reference compound.

2.2. Binding studies

Competition binding experiments with the newly synthesized 8-bicycloalkyl-CPFPX derivatives (hereinafter designated as 1-NBX, 2-NBX, 7-NBX and 1-NBXOF, for details see Tab. 1) and CPFPX as reference compound were performed using membranes from CHO-K1 cells stably transfected with the human A_1R or $A_{2A}R$. The results of these experiments as well as the calculated and/or experimental partition coefficients (clogP/logP) of the different compounds are summarized in Table 1.

Table 1. Calculated (clogP) and measured (logP) lipophilicity and inhibitory constants (K_i) of the new CPFPX derivatives.

Compound	K_i A_1R [nM][a]	K_i $A_{2A}R$ [nM][b]	clogP / logP
CPFPX	3.9 ± 0.3	131 ± 24	2.16 / 3.08 ± 0.02
1-NBX (**11a**)	2.6 ± 0.2	164 ± 8	2.61 / 3.17 ± 0.11
2-NBX (**11c**)	5.6 ± 2.7	193 ± 54	2.32
7-NBX (**11b**)	4.0 ± 2.2	307 ± 180	2.32
1-NBXOF (**17**)	27 ± 9	1581 ± 34	2.35

All experimental values are given as mean ± SD (n=2-6). [a] determined with [^{3}H]DPCPX (K_d = 2.9 ± 0.6 nM for A_1R and 133 ± 12 nM for $A_{2A}R$) as competing radioligand; [b] determined with [^{3}H]ZM241385 (K_d = 1.3 ± 0.4 nM for $A_{2A}R$) as competing radioligand. Abbreviations: K_d, dissociation constant.

Overall, 1-NBX (**11a**) emerged as the most promising candidate, with significantly higher affinity for the A_1 target receptor (two-tailed t-test, p = 0.0006) and significantly lower affinity for the A_{2A} receptor (two-tailed t-test, p = 0.048) than CPFPX. The higher A_1R affinity of 1-NBX compared to CPFPX and the other compounds examined can most likely be attributed to the shape and exact positioning of its norbornyl group. Thus, the cyclopentyl group in CPFPX exists mainly in an “envelope” conformation, in which four of the carbons form the corners of a flat envelope, and the fifth carbon represents the apex of a triangular flap that projects at an angle of about 120° from the body of the envelope[28]. While any of the carbons can take the out-of-plane position in cyclopentane, the bridging carbon in norbornane is locked in this position (Fig. 2). In 1-NBX, the norbornyl group is positioned in a way that the ”locked” cyclopentyl ring always faces the receptor, which appears to be the optimal conformation for binding and likely explains the improved affinity compared to CPFPX with a flexible cyclopentyl ring. Conversely, the surface facing the receptor in 2-NBX (**11c**), can either be the preferred cyclopentyl (2-*endo*-norbornyl isomer) or the less favorable cyclohexyl (2-*exo*-norbornyl isomer) ring, which may account for its reduced affinity compared to 1-NBX. Similarly, the higher affinity of 1-NBX compared to 7-NBX (**11b**) can most likely be explained by the fact that the 7-norbornyl isomer can only bind with the less favorable cyclohexyl ring facing the receptor.

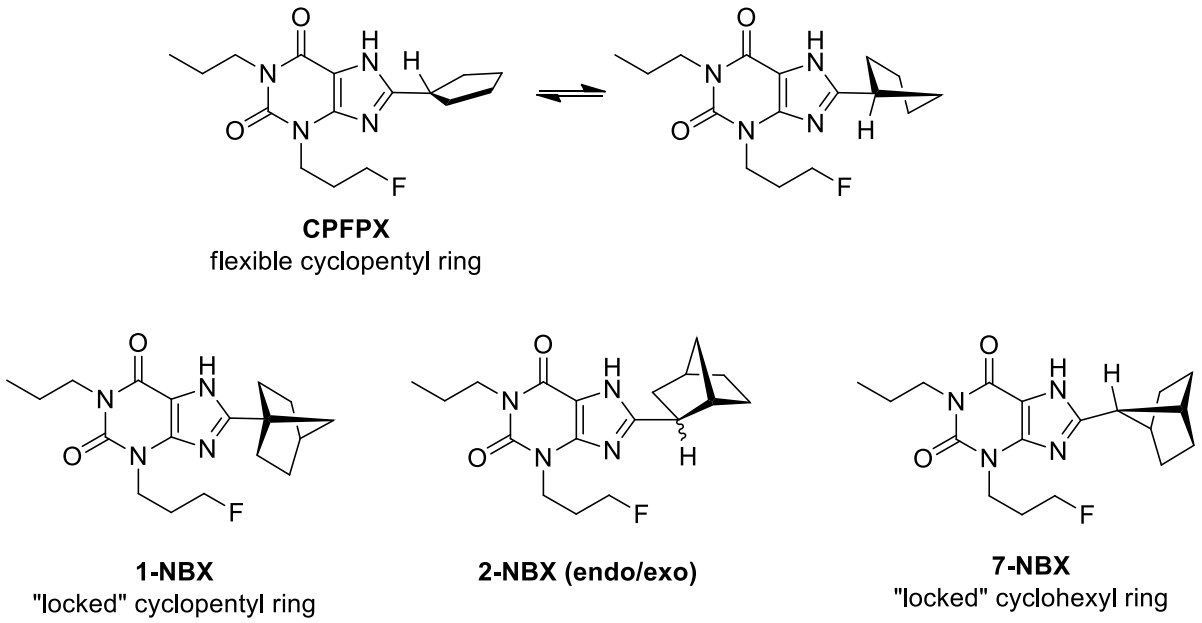

Figure 2: Conformations of CPFPX and the norbornyl derivatives evaluated in the present work.

As expected from earlier studies, 1-propyl substitution at *N*-1 and 3-fluoropropyl substitution at *N*-3 of the xanthine scaffold proved to be optimal for A_1R binding. Thus, replacement of the *N*-3 propyl group with a longer-chain substituent containing an ether function, as in the case of 1-NBXOF (**17**), led to a drastic reduction in affinity (Tab. 1). Finally, prediction of the partition coefficients between octanol and water for the different compounds indicated a relatively narrow range of lipophilicity, with clogP values between 2.16 for CPFPX and 2.61 for 1-NBX (Tab. 1). The slightly higher lipophilicity of 1-NBX compared to CPFPX was further confirmed by determination of experimental partition coefficients (Tab. 1), which demonstrated that both compounds have logP values in the range considered optimal for development of PET neurotracers[29].

2.3. In vitro permeability assays

The in vitro penetration of [^{18}F]1-NBX and [^{18}F]CPFPX across biological membranes was compared by permeability assays with Caco-2 cell monolayers (Fig. 3), which have been shown to provide acceptable predictions of BBB passage for passive diffusion compounds[30]. As expected based on the difference in lipophilicity described above, the apical-to-basolateral permeability coefficient of [^{18}F]1-NBX (6.9±2.9 × 10^{-5} cm/s) was slightly higher than that of the parent compound [^{18}F]CPFPX (5.9±1.9 × 10^{-5} cm/s), although this difference did not reach statistical significance (p=0.053). Nevertheless, these results indicate that the passive permeability of [^{18}F]1-NBX is at least comparable to that of [^{18}F]CPFPX, which has already been shown to exhibit sufficient BBB-penetration for in vivo imaging. In addition, compounds with in vitro permeability coefficients above 5 × 10^{-6} cm/s are generally considered as promising candidates for development of PET neurotracers[31], suggesting that passive penetration of [^{18}F]1-NBX across the BBB should also be sufficient for brain imaging.

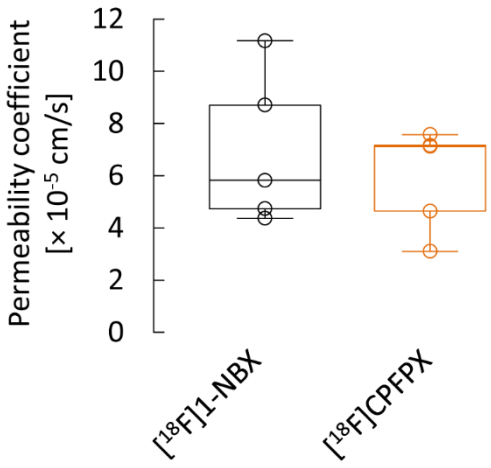

Figure 3: Permeability of [^{18}F]1-NBX and [^{18}F]CPFPX across Caco-2 cell monolayers grown on gelatin-coated cell culture inserts. Shown are apical-to-basolateral permeability coefficients (n=5 per tracer) for the cell layer determined in experiments with transepithelial electrical resistance (TEER) values of at least 600 Ω × cm^2. Boxplots indicate median, 25th and 75th percentile (box), minimum and maximum values (whiskers) and individual data points (dots). Note that there was no significant difference between the results obtained for the two tracers, as determined by a two-tailed t-test (p=0.053).

2.4. In vitro autoradiography and radioligand binding studies

Next, the binding characteristics of [^{18}F]1-NBX ([^{18}F]**11a**) were evaluated by in vitro autoradiography using horizontal rat brain slices. As illustrated in Fig. 4A, the regional radioactivity distribution obtained was consistent with the well-established expression pattern of A_1R in rat brains[32] and the cerebral distribution of [^{18}F]CPFPX in previous studies[8, 33] with most pronounced accumulation in hippocampus, thalamus, cerebellum and neocortex. In addition, the non-displaceable binding in heterologous blocking experiments with 1 µM DPCPX, which should provide a measure for the sum of non-specific and off-target binding, amounted to only 5% of the binding observed in experiments without DPCPX and showed a homogenous brain distribution (Fig. 4B), suggesting that it was mainly due to non-specific binding. Based on these findings, roughly 95% of the total binding of [^{18}F]1-NBX in rat brain slices could be attributed to A_1R-specific on-target binding, which is comparable to the degree of specific binding (~93%) observed in previous *in vitro* studies with [^{18}F]CPFPX[33a].

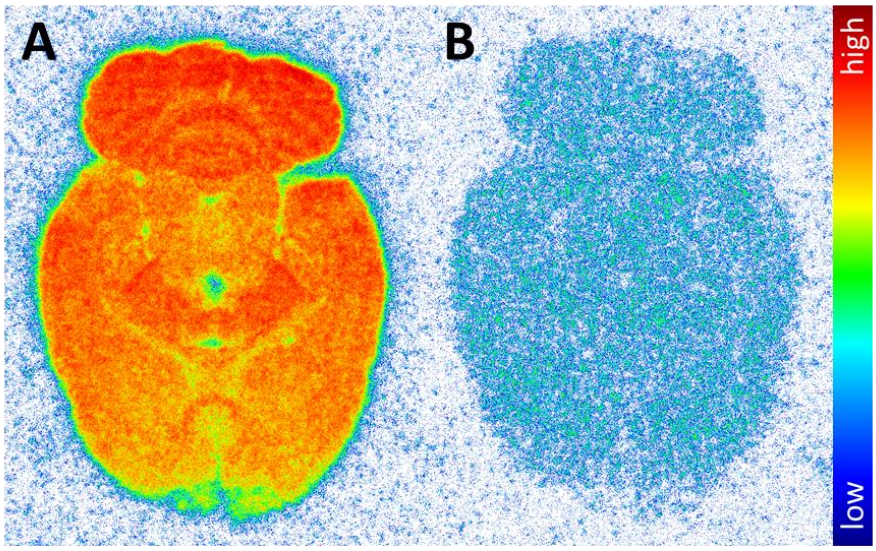

Figure 4: In vitro autoradiography with [^{18}F]1-NBX in horizontal rat brain slices. Regions with high or intermediate tracer binding are shown in red or yellow, while regions with low or no tracer binding are shown in green or blue, respectively. (A) Total binding, (B) binding in the presence of 1 µM DPCPX. The sum of non-specific and off-target binding observed in the presence of DPCPX amounted to about 5% of total binding.

To further confirm these results, additional radioligand binding studies were performed with membranes from A_1R-transfected CHO-K1 cells (CHO-A_1R) and the corresponding non-transfected wildtype cell line (CHO-WT). As illustrated in Fig. 5A, total binding of [^{18}F]1-NBX to CHO-WT membranes was roughly 90% lower than total binding to CHO-A_1R membranes. In addition, while DPCPX significantly reduced binding to CHO-A_1R membranes, it had no effect on the binding to CHO-WT membranes. Finally, the degree of non-displaceable binding to CHO-A_1R membranes observed in the presence of DPCPX was comparable to the degree of total binding to CHO-WT membranes, indicating that most or all of the displaceable binding was due to interaction with A_1Rs. Similar results were obtained in analogous experiments with [^{18}F]CPFPX, although this radioligand showed even lower total binding to CHO-WT membranes and non-displaceable binding to CHO-A_1R membranes, respectively (Fig. 5B). While these differences between the two radioligands did not reach statistical significance, they are in line with the slightly higher lipophilicity of [^{18}F]1-NBX and indicate that it could result in a moderate increase of non-specific binding compared to [^{18}F]CPFPX.

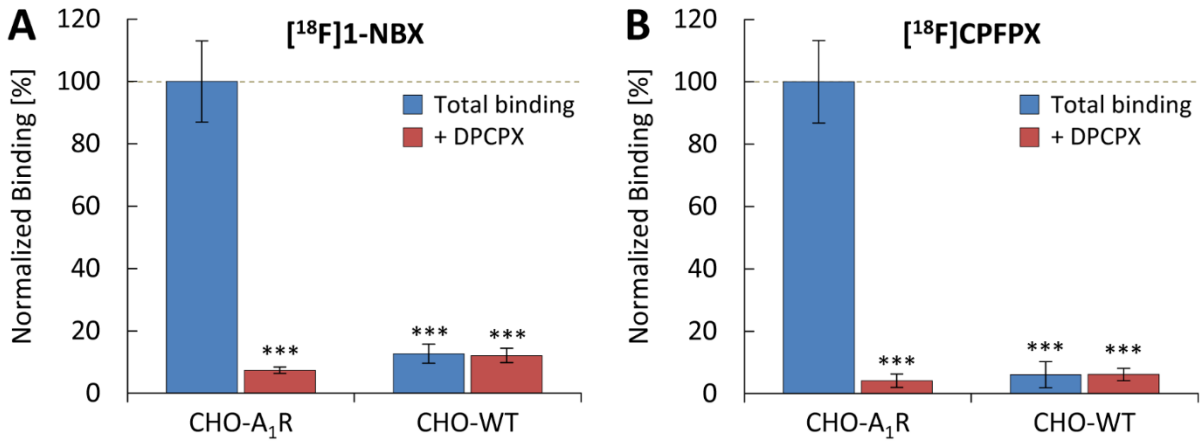

Figure 5: Comparison of tracer binding to membranes from A_1R-transfected (CHO-A_1R) and non-transfected (CHO-WT) CHO-K1 cells. Immobilized membrane homogenates were incubated with (A) [^{18}F]1-NBX or (B) [^{18}F]CPFPX in the absence (total binding) or presence (+ DPCPX) of 2 µM DPCPX and the bound radioactivity after 70 min was normalized to the mean values observed with CHO-A_1R membranes. Asterisks denote statistically significant differences ($p<0.001$) compared to total radioligand binding to CHO-A_1R membranes, as determined by a one-way ANOVA followed by Tukey's post hoc test. Data are shown as mean ± SD (n=4-7).

2.5. Metabolism studies

2.5.1. Rate of microsomal metabolism

Next, the metabolic stability of the novel A_1R ligands was determined in human liver microsomes and compared with that of CPFPX and DPCPX (Fig. 6). Results of previous studies have demonstrated that xanthine-derived adenosine receptor ligands are primarily metabolized by the P450 cytochrome system in the liver[12b] and that the scaled microsomal clearance shows good agreement with the in vivo systemic clearance[10]. As illustrated in Fig. 6, the stability of 1-NBXOF in microsomal assays was comparable to that of CPFPX and DPCPX, whereas metabolism of 1-NBX, 2-NBX and 7-NBX was significantly faster. However, while a high stability towards hepatic metabolism can increase BBB-penetration of PET tracers through higher plasma concentrations, the brain uptake and imaging performance of xanthine derived radioligands have been shown to be primarily governed by affinity, as discussed above. As such, the more favorable stability of 1-NBXOF compared to 1-NBX would most likely be offset by its considerably lower affinity, making this ligand a poor candidate for tracer development. Conversely, while the lower stability of 1-NBX in the microsomal assays warrants consideration, it does not necessarily preclude the application of [^{18}F]1-NBX as PET imaging agent. Thus, as exemplified by the parent compound [^{18}F]CPFPX, even tracers with rapid hepatic clearance can be suitable for brain imaging, provided that peripheral metabolism is not associated with the formation of BBB-penetrating lipophilic radiometabolites. Accordingly, further experiments were performed to elucidate the identity and lipophilicity of metabolites formed during incubation of human liver microsomes with 1-NBX.

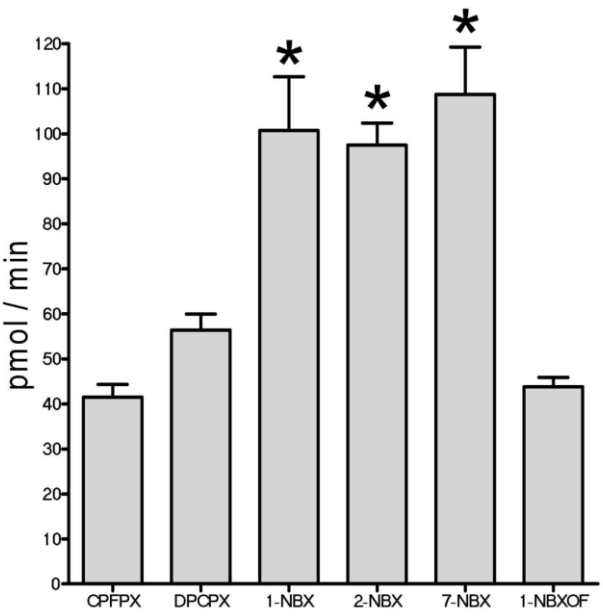

Figure 6: Rate of metabolism of the novel 8-bicycloalkyl-derivatives and the reference compounds CPFPX and DPCPX in human liver microsomes. Asterisks denote statistically significant differences compared to the reference compounds ($p<0.05$), as determined by a one-way ANOVA followed by Tukey's post hoc test. Data are shown as mean ± SD (n = 2-4).

2.5.2. LC-MS Studies of Microsomal 1-NBX Metabolites

To obtain insight into the exact hepatic fate of 1-NBX, the microsomal metabolites formed after incubation for one hour were analyzed by LC-ESI-MS. Since no fragmentation of 1-NBX was observed at cone voltages below 60 V, spectra recorded at 50 V were used to identify the type of functionalization for the different metabolites, while a cone voltage of 185 V was chosen to obtain fragmentation spectra of the metabolites. A plausible fragmentation route for 1-NBX is illustrated in Fig. 7. The interpretation of the fragments is based on the results of previous work[12a].

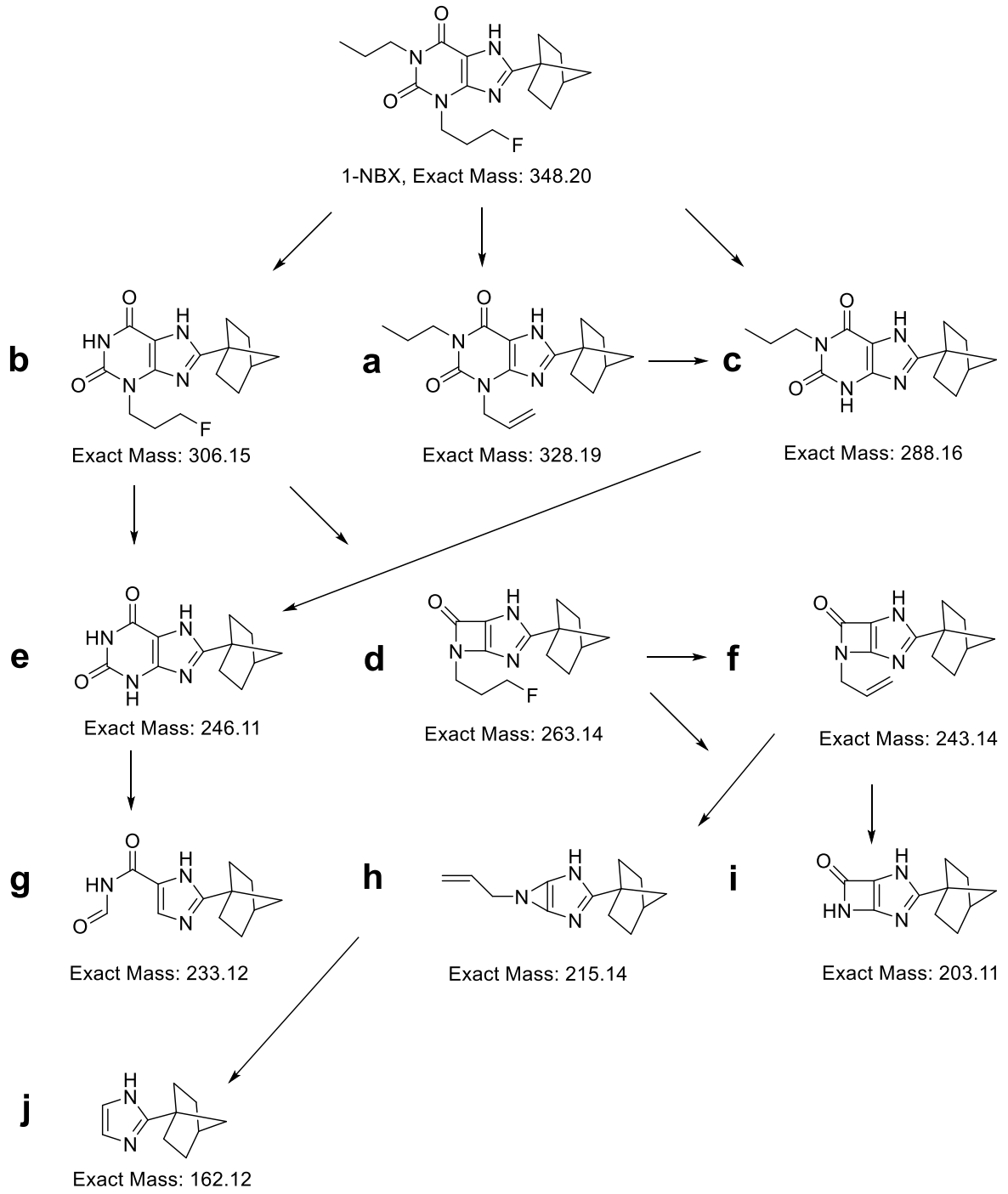

Figure 7: Base fragments (a–j) for interpretation of the in-source fragmentation pathways of 1-NBX.

Fig. 8 shows a typical UV trace of an LC-MS experiment performed with the microsomal metabolite fraction obtained after incubation for one hour, as well as the MS spectra of the most prominent peak P1 (inset A) and of 1-NBX (inset B). About 90% of the peaks obtained in the chromatogram could be identified and unambiguous mass numbers could be assigned to all peaks numbered in this figure and reported in table 2. In addition, none of the peaks reported in table 2 were present in control incubations containing all reactants except 1-NBX. Based on the results obtained in the LC-MS experiments, hydroxylation was the preferred (85%) functionalization of 1-NBX (Tab. 2), which is in line

with the results obtained for [^{18}F]CPFPX and other xanthines in previous studies[12a, 34]. In addition, one oxo- and one unsaturated metabolite formed by functionalization of the norbornyl moiety could be detected. The two most prominent peaks P1 and P2 corresponded to compounds in which the norbornyl residue was hydroxylated and had almost indistinguishable MS spectra. Thus, similar to CPFPX[12a], the substituent on the C8 atom of the xanthine scaffold represents the predominant site for metabolic functionalization of 1-NBX, while metabolites hydroxylated at the *N*-1 propyl residue are formed in much smaller quantities. Moreover, neither metabolites functionalized at the *N*-3 fluoropropyl moiety nor $[M+H]^+$ ions equivalent to despropyl 1-NBX (m/z 289) or desfluoropropyl 1-NBX (m/z 307) could be detected, indicating that 1-NBX is not metabolized by oxidative modification of C1 of the 1-propyl or 3-fluoropropyl groups. Taken together, these findings suggest that 1-NBX behaves similar to CPFPX in that it undergoes extensive hydroxylation and oxidation by liver microsomes but is resistant to enzymatic *N*-dealkylation, which represents the major pathway for hepatic metabolism of naturally occurring methylxanthines like theophylline[35]. Accordingly, the *N*3-[^{18}F]fluoropropyl moiety in [^{18}F]1-NBX should also be resistant to cleavage and further metabolism, so that hepatic clearance of this radioligand can be expected to result in exclusive formation of ^{18}F-labeled metabolites. While this would prevent significant radioactivity deposition in bone due to radiodefluorination, the radiometabolites formed could potentially interfere with the quantification of A_1R-specific binding.

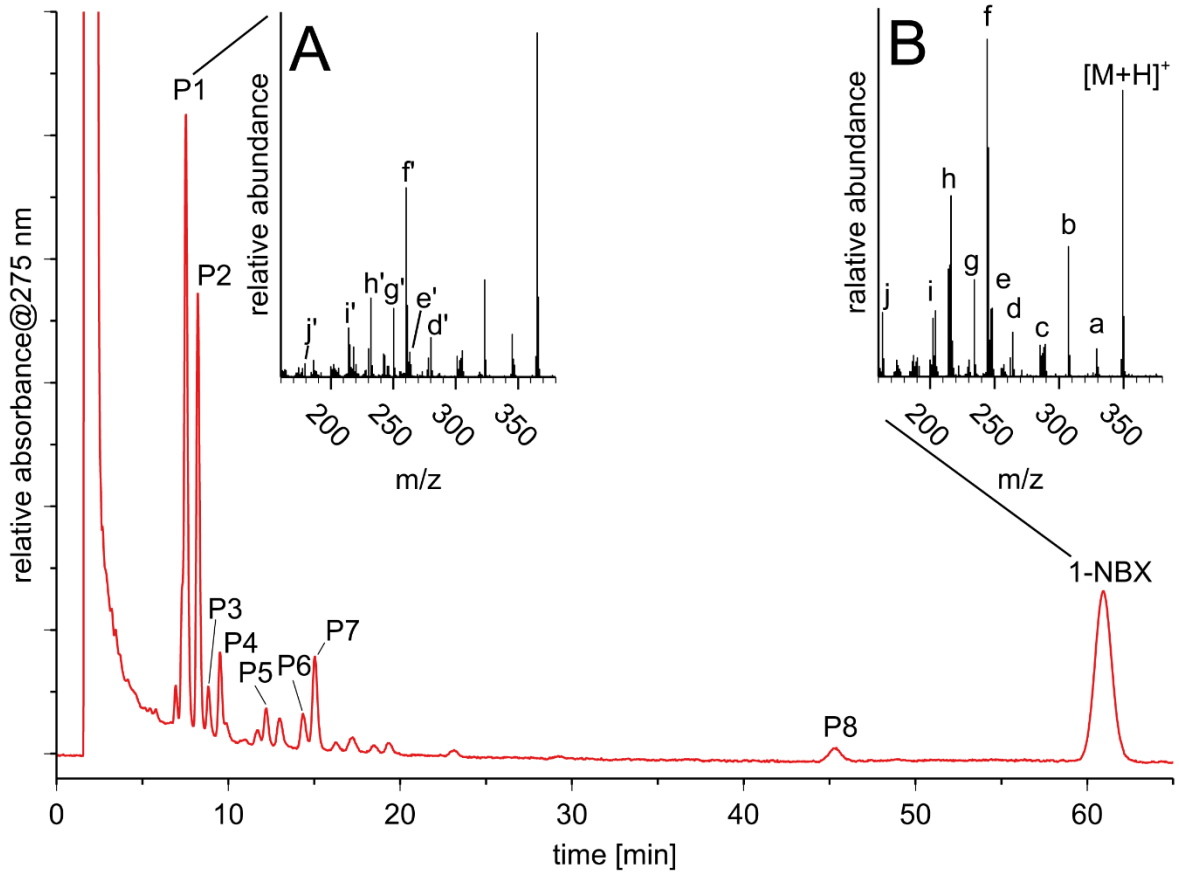

Figure 8: Analysis of 1-NBX metabolites formed in human liver microsomes by HPLC (Kromasil 5RP18 4.6 x 250 mm column, 0.2 % HOAc in CH_3CN/H_2O (35/65, UV@275 nm, flow rate 1 mL / min). Inset A: ESI-MS spectrum of the metabolite P1 at a cone voltage of 185 V. Key fragments corresponding to the functionalized (hydroxylated) fragments of 1-NBX in inset B are designated by letters with an apostrophe. Inset B: ESI-MS spectrum of 1-NBX at a cone voltage of 185 V. Letters above the peaks refer to the interpretation presented in Figure 7.

Importantly however, based on their retention behavior on a reverse phase column, there was a large difference between the lipophilicity of 1-NBX and its metabolites, with the metabolites being substantially more hydrophilic (Fig. 8 and Tab. 2). As such, the corresponding radiometabolites formed by peripheral metabolism of [^{18}F]1-NBX would not be expected to cross the BBB and directly interfere with in vivo application of this radioligand for brain imaging. Nevertheless, while previous studies indicate that microsomal assays do indeed closely recapitulate the metabolism of xanthine-based A_1R-(radio)ligands in animal models and human subjects[10, 12a], they provide limited insight into the exact proportion of metabolites formed in vivo or their brain penetration. Accordingly, further studies to assess the in vivo metabolism, BBB-penetration and binding properties of [^{18}F]1-NBX and its metabolites in preclinical species and/or human tissues will clearly be required to firmly establish the suitability of this radioligand for A_1R-specific PET imaging.

Table 2. Interpretation of peaks P1 – P8 found after "in source" fragmentation of microsomal metabolite fractions of 1-NBX as exemplified in Figure 7 (90.2 % of peaks identified).

Peak	k' (R_t [min])	Interpretation (fragments)	Functionalization		Fraction in the chromatogram [%]
			Type	Site	
1	3.8 (7.5)	+OH, -H: (d, e, f, g, h, i, j)	„-OH“	@Norbornyl	40.0
2	4.2 (8.2)	+OH, -H: (d, e, f, g, h, i, j)	„-OH“	@Norbornyl	25.3
3	4.6 (8.8)	+OH, -H: (d, e, f, g)	„-OH“	@Norbornyl	2.6
4	5.1 (9.5)	+OH, -H: (d, e, f, g)	„-OH“	@Norbornyl	6.8
5	6.8 (12.2)	+O, -2H: (d, e, f, h, i)	„=O“	@Norbornyl	2.2
6	8.2 (14.3)	+OH, -H: (a, c)	„-OH“	@Propyl	2.4
7	8.7 (15.0)	+OH, -H: (a, c)	„-OH“	@Propyl	7.5

8	28.0 (45.4)	-2H: (f, g, h, i)	„=“	@Norbornyl	3.4

Abbreviations: k’, capacity factor; R_t, retention time.

3. Conclusion

1-NBX, a norbornyl-substituted CPFPX derivative, was identified as a potent and selective A_1R ligand with higher affinity than DPCPX, the current gold standard of xanthine-based A_1R ligands. In addition, in vitro autoradiography with [^{18}F]1-NBX demonstrated a high degree of A_1R-specific binding (95%). As such, our findings lay a solid foundation for development of improved radiotracers for A_1R PET imaging, although further binding studies with human tissues and a rigorous preclinical in vivo evaluation in multiple models with appropriate controls will be required to fully realize the clinical utility of [^{18}F]1-NBX. In addition, based on the relatively low stability of 1-NBX in the microsomal assays, development of metabolically stabilized derivatives could represent a promising approach to further improve the imaging properties of [^{18}F]1-NBX. Thus, even though our findings indicate that peripheral metabolism of [^{18}F]1-NBX is unlikely to result in the formation of BBB-penetrating lipophilic radiometabolites, it could prevent imaging of peripheral A_1Rs and/or reduce brain delivery of intact tracer.

4. Experimental Section

4.1. General information

Unless noted otherwise, all reactions were carried out under argon at ambient temperature (22 ± 2°C) in oven-dried glassware. Standard inert atmosphere techniques were used in handling all air and moisture sensitive reagents. Melting points were measured on a FP62 - Melting Point Meter (Mettler Toledo, Gießen, Germany) and are uncorrected. >95% purity of all compounds was confirmed by NMR and elemental analysis.

4.2. Solvents and reagents

Solvents were either purchased in sufficient purity (MerckKGaA, Darmstadt, Germany) or purified and dried by standard methods[36] . All chemicals used for the syntheses were commercially available (Merck, Taufkirchen, Germany; Activate Scientific, Prien, Germany; ABCR, Karlsruhe, Germany) or were prepared as described in the text. 5,6-Diamino-1-(2,4-dimethoxybenzyl)-3-propyluracil (**6**) was prepared as described previously[24].

4.3. Spectroscopy

^{1}H-, ^{13}C-, and ^{19}F-NMR spectra were recorded at 400.13, 100.61, and 376.49 MHz using a Bruker Avance Neo 400 instrument (Bruker Bio Spin GmbH, Rheinstetten, Germany) in 5% solution at 298 K. Chemical shifts (δ) are reported in parts per million (ppm). Residual solvent signals are δ_H = 7.28, δ_C = 77.0 for

$CDCl_3$, δ_H = 2.51 and δ_C = 40.0 for DMSO-d_6. Bruker's implemented reference (CCl_3F, δ = 0.00 ppm) was used in all ^{19}F experiments. The ^1H-NMR spectra are reported as follows: δ/ppm, multiplicity, coupling constant *J*/Hz (where appropriate), number of protons, assignment. The following abbreviations and their combinations are used when reporting NMR data: s = singlet, d =doublet, t = triplet, q = quartet, p = pentet, sx = sextet, m = multiplet and s_{br} = broad singlet. NMR signals were assigned based on information from additional two-dimensional experiments (COSY, gHSQC, gHMBC, NOESY). Coupling constants *J* (in Hertz) for protons are given in the form $^nJ(^1H, X)$, those for carbons as $^nJ(^{13}C,^{19}F)$. All ^{13}C- and ^{19}F-NMR spectra were recorded under ^1H-broadband decoupling (CPD). Compound names were generated by ChemBioDraw™ (CambridgeSoft) following IUPAC nomenclature. Numbering of the bicyclo[2.2.1]heptane (norbornane) scaffold is shown below:

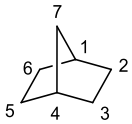

Low-resolution mass spectra were obtained in electrospray ionization (ESI positive) mode with a Thermo Finnigan Surveyor mass spectrometer (Thermo Fisher Scientific GmbH, Dreieich, Germany). The analytes were dissolved in methanol (about 1 mg / mL) and injected directly through a valve on the ionisation interface. The flow rate of the eluent (2% acetic acid in methanol/water, 50/50, v/v) was 200 µL/min. Reported are the m/z-values of the pseudo-ion $[M + H]^+$.

High resolution mass spectrometry was performed by the Central Division of Analytical Chemistry at the Forschungszentrum Jülich. Elemental analyses were performed by HEKAtech GmbH (Wegberg, Germany). Analyses indicated by the symbols of the elements are within ± 0.4% of the theoretical values.

4.4. Chromatography

Thin layer chromatography (TLC) analyses were performed for all reactions to monitor the reaction progress and to estimate the purity of the obtained products. The respective eluent was selected so that the R_f values of the individual compounds ranged from 0.2 to 0.8. Chromatograms were visualized by detection under UV light using silica coated TLC aluminium sheets with fluorescent indicator (ALUGRAM SIL G/UV_{254} Macherey-Nagel GmbH, Düren, Germany) and / or by iodine staining.

For flash chromatography (FC), a Büchi Pure C-815 flash chromatography system (BÜCHI Labortechnik AG, Flawil, Switzerland) equipped with multisignal (UV / ELSD) detection and FlashPure silica cartridges (particle size 40 µm) as stationary phase were employed. Solvent proportions are indicated in a volume / volume ratio.

Analytical HPLC was performed on a HPLC system (Knauer, Berlin, Germany) consisting of an Azura P 6.1L pump, Rheodyne 7725i injection valves equipped with the original 20 µL steel loops, and an Azura UVD 2.1S UV detector coupled in series with a HERM LB 500 2'' NaI radiation detector with digital

signal transmission (Berthold Technologies, Bad Wildbad, Germany). Data acquisition was performed with Knauer ClarityChrom 8 software.

Semi-preparative HPLC was performed on a HPLC system consisting of a 40P Pump (Knauer, Berlin, Germany), a Rheodyne 7725i injection valve equipped with a 2 mL steel loop, and an Azura UVD 2.1S UV detector coupled in series with a custom-made Geiger counter. Data acquisition was performed with the custom JuHPLC software.

4.5. Chemistry

2-Bromobicyclo[2.2.1]heptane-1-carboxylic acid (2)[20]

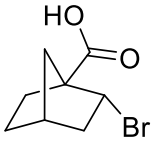

At ambient temperature and under magnetic stirring, bromine (2.82 mL, 8.8 g, 55 mmol) followed by PCl_3 (100 µL, 157.4 mg, 1.15 mmol) were added to 2-norbornanecarboxylic acid (**1**) (> 95% pure, 6.4 g, 45.7 mmol). The mixture was stirred at 85 °C for 7 h, an additional amount of bromine (1.28 mL, 4.0 g, 25 mmol) was added and the mixture was stirred at 85 °C for another 3 h. The mixture was then poured onto water (250 mL) and diethyl ether (50 mL), and an additional amount of diethyl ether (100 mL) followed by $Na_2S_2O_4$ (6 g, 34.5 mmol) were added under efficient stirring. The organic layer was separated, washed with water (2 × 50 mL) and brine (50 mL) and dried over Na_2SO_4. The diethyl ether was removed by rotary evaporation and the solid residue was recrystallized twice from dry toluene to afford the title compound (7.8 g, 42.9 mmol, 78%) as colorless crystals, mp 150-151 °C. ^{1}H-NMR (400 MHz, $CDCl_3$) 10.66 (s, 1H, COO*H*), 4.16 (m, 1H, C*H*Br), 2.30 (m, 1H, H^4), 1.71 (m, 8H, CH_2).

Bicyclo[2.2.1]heptane-1-carboxylic acid (3)[21]

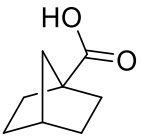

2-Bromobicyclo[2.2.1]heptane-1-carboxylic acid (**2**) (3.2 g, 14.6 mmol, 1.0 equiv) was added to a vigorously stirred suspension of zinc powder (<10 micron, 9.6 g, 146 mmol, 10 equiv) in acetic acid (13.5 mL). A second portion of acetic acid (13.5 mL) was used to rinse the walls of the flask and the reaction mixture was brought to a gentle reflux in an oil bath for 5 h. The reaction mixture was cooled to room temperature, filtered through a pad of Celite on a plastic sintered funnel, and washed with acetic acid (20 mL) and ethyl acetate (30 mL). The filtrate was concentrated under reduced pressure, diluted with water (20 mL), and stirred vigorously to induce precipitation. The precipitate was collected by filtration, washed with water, and dried under reduced pressure for 18 h. Pentane (20 mL) was then added and the mixture was stirred vigorously for 20 min, during which a fine white precipitate started to form. After standing at 5 °C overnight, the precipitate was collected by filtration, washed with

pentane (10 mL), and air dried to afford the title compound (1.67 g, 81%) as a white solid, mp 105-107 °C. ^{1}H-NMR (400 MHz, $CDCl_3$): δ 1.32-1.42 (m, 2H, CH_2), 1.53-1.66 (m, 4H, CH_2), 1.67-1.79 (m, 2H, CH_2), 1.89-2.01 (m, 2H, CH_2) 2.35 (m, 1H, H^4), 11.38 (s_{br}, 1H, COO*H*, D_2O exchange). ^{13}C-NMR (101 MHz, $CDCl_3$): δ 30.0 (*C*H_2), 32.9 (*C*H_2), 37.8 (*C*^{4}H), 42.3 (*C*H_2), 52.1 (*C*^{1}), 183.6 (*C*OOH).

Bicyclo[2.2.1]heptane-7-carboxylic acid (5)[37]

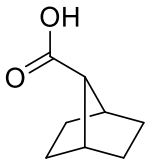

Under a nitrogen atmosphere, freshly cleaned lithium wire (0.21 g, 30 mmol) was added to a solution of 4-4'-di-*tert*-butylbiphenyl (8.25 g, 31 mmol) in anhydrous THF (70 mL). The resulting mixture was stirred at room temperature for 15 min to initiate the reaction, and then cooled in an ice bath and stirred for an additional 4 h. The resulting blue solution was cooled with a dry ice/acetone bath and a solution of 7-bromo-bicyclo[2.2.1]heptane (2.0 g, 11.4 mmol) in anhydrous THF (5 mL) was added in one portion. The reaction mixture was stirred for 20 minutes, during which the blue color changed to orange. Solid dry ice was then added, upon which the reaction mixture became colorless. The dry ice/acetone bath was removed and the reaction mixture was stirred for 2 h and allowed to reach room temperature. 2.5 N aqueous NaOH (200 mL) was added and the mixture was stirred for 5 min. The layers were separated and the aqueous layer was washed with diethyl ether (2 × 50 mL), acidified by addition of concentrated HCl and extracted with diethyl ether (3 × 75 mL). The combined organic layers were dried over anhydrous Na_2SO_4 and concentrated to afford the title compound (1.54 g, 11.1 mmol, 96%) as a white solid, mp = 74-75 °C. ^{1}H-NMR (400 MHz, $CDCl_3$): δ 1.23- 1.34 (m, 4H), 1.64 (d, *J* = 8.4 Hz, 2H), 1.83 (d, *J* = 8.4 Hz, 2H), 2.49 (s, 3H), 10.83 (s_{br}, 1H, COO*H*, D_2O exchange). ^{13}C-NMR (101 MHz, $CDCl_3$): δ 28 (*C*H_2), 29.9 (*C*H_2), 39.2 (*C*H), 53.7 (*C*H), 180.2 (*C*OOH).

General procedure A: Synthesis of *N*-3 DMB protected xanthines 7a–c

4-Methylmorpholine (1100 µL, 10 mmol) was added under argon to a stirred solution of the respective norbornanecarboxylic acid (**1**, **3** or **5**) (10 mmol) in dry DMF (40 mL). The clear solution was cooled to 0-5 °C and isobutylchloroformate (1300 µL, 10 mmol) was slowly added via a syringe. The resulting cloudy mixture was stirred for 10 min, after which 5,6-diamino-1-(2,4-dimethoxybenzyl)-3-propyluracil (**6**) (3.34 g, 10 mmol) was added at 0-5 °C in five portions over 10 min. The mixture was stirred at 0-5 °C for 1 h and at ambient temperature overnight. The mixture was then poured into ice/water (250 mL), stirred for 1 h and cooled overnight, which gave a gelatinous colorless solid that was collected by filtration and washed with water (50 mL) and diethyl ether (50 mL). The solid (intermediate amide, ± 8 mmol) was suspended in a mixture of aqueous 2 N NaOH (40 mL) and dioxane (25 mL) and stirred at 85 °C for 5 h (after 0.5 h a clear solution had formed; TLC: ethyl acetate/hexane, 50/50, v/v). The solution was poured into ice/water (100 mL), the resulting mixture was acidified to pH 4-5 with 5 N

aqueous HCl and stirred for 1 h. After cooling for 2 h at 5 °C, the resulting precipitate was collected by filtration, washed with water and a small volume of diethyl ether, and dried in an oven at 100 °C to afford the desired xanthines (**7a**-**c**) as colorless solids.

3-(2,4-Dimethoxybenzyl)-8-(1-norbornyl)-1-propyl-1*H*-purine-2,6(3*H*,7*H*)-dione (**7a**)

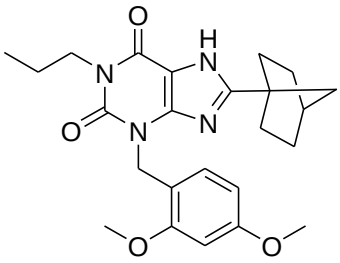

Colorless crystals, 63%, mp 254-255 °C. ^{1}H-NMR (400 MHz, DMSO-d_6): δ 0.88 (t, $^{3}J_{H\text{-}H}$ = 7.5 Hz, 3H, CH_3), 1.26 – 1.45 (m, 2H, CH_3-CH_2), 1.49 -1.96 (m, 10H, 1-Nb-CH_2), 2.32 (s_{br}, 1H, 1-Nb-CH), 3.74 (s, 3H, 4-OCH_3), 3.78 – 3.93 (m, 2H, N^{1}-CH_2), 3.84 (s, 3H, 2-OCH_3), 5.07 (s, 2H, Ph-CH_2), 6.41 (dd, $^{3}J_{H\text{-}H}$ = 8.4 Hz, $^{4}J_{H\text{-}H}$ 2.4 Hz, 1H, Ph-H^5), 6.59 (d, $^{4}J_{H\text{-}H}$ = 2.3 Hz, 1H, Ph-H^3), 6.73 (d, $^{3}J_{H\text{-}H}$ = 8.4 Hz, 1H, Ph-H^6), 13.12 (s_{br}, 1H, N^{7}-H). ^{13}C-NMR (101 MHz, DMSO-d_6): δ 11.6 (CH$_3$), 21.3 (CH_3-CH$_2$), 30.2 (1-Nb-CH$_2$), 34.9 (1-Nb-CH$_2$), 37.7 (1-Nb-CH), 41.5 (Ph-CH$_2$), 43.8 (N^{1}-CH$_2$), 47.6 (1-Nb-C), 55.7 (4-OCH$_3$), 56.0 (2-OCH$_3$), 68.5 (1-Nb-CH$_2$), 98.9 (Ph-C^3), 105.0 (Ph-C^5), 107.0 (C^5), 117.2 (Ph-C^1), 127.3 (Ph-C^6), 148.3 (C^4), 151.2 (C^2), 154.4 (C^6), 157.9 (C^8), 158.0 (Ph-C^2), 160.1 (Ph-C^4). Elemental analysis calcd for $C_{24}H_{30}N_4O_4$: C 63.73, H 6.90, N 12.78; found: C 63.80, H 6.81, N 12.82. HRMS (ESI) *m*/*z* calcd for $C_{24}H_{30}N_4O_4$+H$^+$: 439.2339 [*M*+H]$^+$; found: 439.2342.

3-(2,4-Dimethoxybenzyl)-8-(7-norbornyl)-1-propyl-1*H*-purine-2,6(3*H*,7*H*)-dione (**7b**)

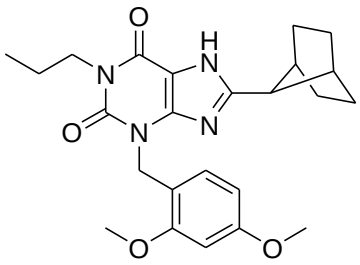

Colorless solid, 55%, mp 255 °C. ^{1}H-NMR (400 MHz, DMSO-d_6): δ 0.88 (t, $^{3}J_{H\text{-}H}$ = 7.5 Hz, 3H, CH_3), 1.06 – 1.34 (m, 4H, 7-Nb-CH_2), 1.44 -1.77 (m, 6H, 7-Nb-CH_2 + CH_3-CH_2), 2.63 (s_{br}, 2H, 7-Nb-CH), 2.80 (s, 1H, 7-Nb-CH), 3.73 (s, 3H, 4-OCH_3), 3.76 – 3.96 (m, 2H, N^{1}-CH_2), 3.83 (s, 3H, 2-OCH_3), 5.08 (s, 2H, Ph-CH_2), 6.40 (dd, $^{3}J_{H\text{-}H}$ = 8.4 Hz, $^{4}J_{H\text{-}H}$ 2.4 Hz, 1H, Ph-H^5), 6.59 (d, $^{4}J_{H\text{-}H}$ = 2.3 Hz, 1H, Ph-H^3), 6.73 (d, $^{3}J_{H\text{-}H}$ = 8.4 Hz, 1H, Ph-H^6), 13.10 (s_{br}, 1H, N^{7}-H). ^{13}C-NMR (101 MHz, DMSO-d_6): δ 11.6 (CH$_3$), 21.4 (CH_3-CH$_2$), 28.0 (7-Nb-CH$_2$), 29.9 (7-Nb-CH$_2$), 40.0 (7-Nb-CH), 41.4 (Ph-CH$_2$), 42.6 (N^{1}-CH$_2$), 48.7 (7-Nb-CH), 55.7 (4-OCH$_3$), 56.0 (2-OCH$_3$), 98.8 (Ph-C^3), 104.9 (Ph-C^5), 106.7 (C^5), 117.3 (Ph-C^1), 127.5 (Ph-C^6), 148.4 (C^4), 151.1 (C^2), 154.4 (C^6), 157.9 (C^8), 158.0 (Ph-C^2), 160.1 (Ph-C^4).). Elemental analysis calcd for $C_{24}H_{30}N_4O_4$: C 63.73, H 6.90, N 12.78; found: C 63.76, H 6.92, N 12.80. HRMS (ESI) *m*/*z* calcd for $C_{24}H_{30}N_4O_4$+H$^+$: 439.2339 [*M*+H]$^+$; found: 439.2336.

3-(2,4-Dimethoxybenzyl)-8-(2-*endo/exo*-norbornyl)-1-propyl-1*H*-purine-2,6(3*H*,7*H*)-dione (**7c**)

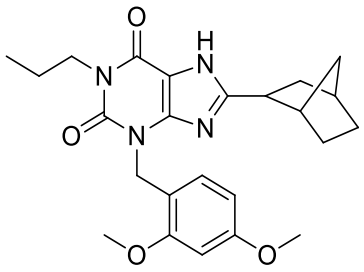

Colorless solid, 72%, mp 222-223 °C. ^{1}H-NMR (400 MHz, DMSO-d_6): δ 0.84 + 0.86 (2t, $^{3}J_{H\text{-}H}$ = 7.4 Hz, 3H, CH_3), 0.95 – 1.61 (m, 8H, CH_3-CH_2, 2-Nb-CH_2), 1.73 – 1.85 (m, 1H, C$^{4'}H$), 1.92 – 1.99 (m, 0.4 H), 2.24 – 2.28 (m, 1H, C$^{1'}H$), 2.36 (s_{br}, 0.5 H), 2.75 – 2.78 (m, 0.4 H), 3.14 – 3.19 (m, 0.6H), 3.71 (s, 3H, 4-OCH_3), 3.81 – 3.86 (m, 5H, N^{1}-CH_2 + 2-OCH_3), 5.03 – 5.13 (m, 2H, Ph-CH_2), 6.37 – 6.41 (m, 1H, Ph-H^5), 6.56 – 6.57 (m, 1H, Ph-H^3), 6.70 – 6.74 (m, 1H, Ph-H^6), 13.09 (s_{br}, 1H, N^{7}-H). ^{13}C-NMR (101 MHz, DMSO-d_6): δ 11.6, 21.3, 24.0, 28.8, 29.4, 29.5, 32.8, 35.7, 36.0, 36.1, 37.0, 40.1, 41.3, 41.5, 42.1, 42.5, 43.0, 55.6, 55.9, 56.0, 98.8, 104.9, 106.9, 117.2, 127.5, 127.6, 148.2, 148.3, 151.1, 156.7, 157.9, 158.0, 160.1. Elemental analysis calcd for $C_{24}H_{30}N_4O_4$: C 63.73, H 6.90, N 12.78; found: C 63.77, H 6.92, N 12.74. HRMS (ESI) *m*/*z* calcd for $C_{24}H_{30}N_4O_4$+H^+: 439.2339 [*M*+H]$^+$; found: 439.2336.

General procedure B: *N*-7 Pom protection, synthesis of xanthines 8a–c

Dry potassium carbonate (152 mg, 1.1 mmol) was added under argon at 60 °C to a stirred suspension of the respective xanthine (**7a**-**c**) (10 mmol) in dry DMF (75 mL). The mixture was stirred for 5 min, after which the xanthine had completely dissolved. POM-Cl (1.87 mL, 13 mmol) was then added and the mixture was stirred at 60 °C for 2-16 h (TLC: ethyl acetate/hexane, 50/50, v/v). After cooling to ambient temperature, the reaction mixture was poured into a stirred ice/water mixture (400 mL) and the resulting semi-solid precipitate was extracted with diethyl ether (2 × 100 mL). The combined organic layers were washed with water (3 × 100 mL) and brine (100 mL), dried over anhydrous Na_2SO_4, and concentrated under reduced pressure to afford the desired pivalates (**8a**-**c**) as yellowish semi-solids in near quantitative yield. Treatment of the solid residues with a small volume of hot methanol followed by cooling and filtration removed yellow impurities and afforded the products as almost colorless crystals.

3-(2,4-Dimethoxybenzyl)-8-(1-norbornyl)-7-pivaloyloxymethyl-1-propyl-1*H*-purine-2,6(3*H*,7*H*)-dione (**8a**)

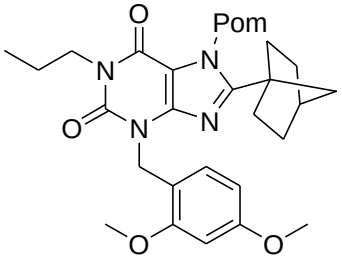

Yellowish crystals, 99%, mp 123-124 °C. ^{1}H-NMR (400 MHz, $CDCl_3$): δ 0.96 (t, $^{3}J_{H\text{-}H}$ = 7.5 Hz, 3H, CH_3), 1.23 (s, 9H, N^7-POM-CH_3), 1.38 – 1.96 (m, 12H, CH_3-CH_2 + 1-Nb-CH_2), 2.39 (s_{br}, 1H, 1-Nb-C*H*), 3.82 (s, 3H, 4-OCH_3), 3.85 (s, 3H, 2-OCH_3), 3.92 – 4.07 (m, 2H, N^1-CH_2), 5.30 (s, 2H, Ph-CH_2), 6.31 (s, 2H, N^7-Pom-CH_2), 6.42 (dd, $^{3}J_{H\text{-}H}$ = 8.4 Hz, $^{4}J_{H\text{-}H}$ 2.4 Hz, 1H, Ph-H^5), 6.48 (d, $^{4}J_{H\text{-}H}$ = 2.3 Hz, 1H, Ph-H^3), 7.15 (d, $^{3}J_{H\text{-}H}$ = 8.4 Hz, 1H, Ph-H^6). ^{13}C-NMR (101 MHz, $CDCl_3$): δ 11.3 (*C*H_3), 21.3 (CH_3-*C*H_2), 27.0 (N^7-Pom-*C*H_3), 30.4 (1-Nb-*C*H_2), 35.2 (1-Nb-*C*H_2), 36.4 (1-Nb-*C*H), 38.8 (N^7-Pom-*C*$(CH_3)_3$), 41.5 (Ph-*C*H_2), 42.8 (1-Nb-*C*H_2), 43.7 (N^1-*C*H_2), 47.9 (1-Nb-*C*), 55.4 (4-O*C*H_3), 55.5 (2-O*C*H_3), 68.5 (N^7-POM-*C*H_2), 98.5 (Ph-C^3), 104.0 (Ph-C^5), 107.1 (C^5), 117.4 (Ph-C^1), 129.5 (Ph-C^6), 148.1 (C^4), 151.2 (C^2), 154.6 (C^6), 158.3 (C^8), 158.6 (Ph-C^2), 160.3 (Ph-C^4), 177.2 (*C*=O). Elemental analysis calcd for $C_{30}H_{40}N_4O_6$: C 65.20, H 7.30, N 10.14; found: C 65.18, H 7.26, N 10.18. HRMS (ESI) *m*/*z* calcd for $C_{30}H_{40}N_4O_6$+H^+: 553.3021 $[M+H]^+$; found: 553.3019.

3-(2,4-Dimethoxybenzyl)-8-(7-norbornyl)-7-pivaloyloxymethyl-1-propyl-1*H*-purine-2,6(3*H*,7*H*)-dione (**8b**)

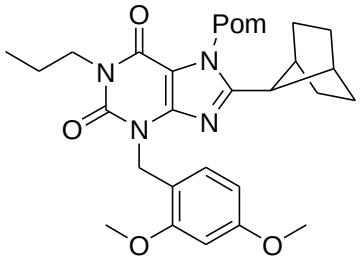

Colorless crystals, 96%, mp 123-124 °C. ^{1}H-NMR (400 MHz, DMSO-d_6): δ 0.86 (t, $^{3}J_{H\text{-}H}$ = 7.5 Hz, 3H, CH_3), 1.14 (s, 9H, N^7-Pom-CH_3), 1.16 – 1.36 (m, 4H, 7-Nb-CH_2), 1.47 – 1.65 (m, 2H, CH_3-CH_2), 1.65 – 1.87 (m, 4H, 7-Nb-CH_2), 2.46 (s_{br}, 2H, 7-Nb-C*H*), 3.04 (s_{br}, 1H, 7-Nb-C*H*), 3.74 (s, 3H, 4-OCH_3), 3.77 – 3.92 (m, 2H, N^1-CH_2), 3.81 (s, 3H, 2-OCH_3), 5.09 (s, 2H, Ph-CH_2), 6.24 (s, 2H, N^7-Pom-CH_2), 6.42 (dd, $^{3}J_{H\text{-}H}$ = 8.4 Hz, $^{4}J_{H\text{-}H}$ 2.4 Hz, 1H, Ph-H^5), 6.57 (d, $^{4}J_{H\text{-}H}$ = 2.3 Hz, 1H, Ph-H^3), 6.85 (d, $^{3}J_{H\text{-}H}$ = 8.4 Hz, 1H, Ph-H^6). ^{13}C-NMR (101 MHz, DMSO-d_6): δ 11.56 (*C*H_3), 21.3 (CH_3-*C*H_2), 27.0 (N^7-Pom-*C*H_3), 28.0 (7-Nb-*C*H_2), 30.0 (7-Nb-*C*H_2), 38.8 (N^7-Pom-*C*$(CH_3)_3$), 41.1 (7-Nb-*C*H), 41.3 (Ph-*C*H_2), 42.8 (7-Nb-*C*H_2), 43.7 (N^1-*C*H_2), 46.1 (7-Nb-*C*H), 55.7 (4-O*C*H_3), 55.9 (2-O*C*H_3), 68.3 (N^7-Pom-*C*H_2), 98.8 (Ph-C^3), 105.0 (Ph-C^5), 107.2 (C^5), 117.5 (Ph-C^1), 128.3 (Ph-C^6), 148.0 (C^4), 151.2 (C^2), 154.6 (C^6), 158.3 (C^8), 158.5 (Ph-C^2), 160.2 (Ph-C^4), 177.2 (*C*=O). Elemental analysis calcd for $C_{30}H_{40}N_4O_6$: C 65.20, H 7.30, N 10.14; found: C 65.24, H 7.33, N 10.10. HRMS (ESI) *m*/*z* calcd for $C_{30}H_{40}N_4O_6$+H^+: 553.3021 $[M+H]^+$; found: 553.3024.

3-(2,4-Dimethoxybenzyl)-8-(2-*endo/exo*-norbornyl)-7-pivaloyloxymethyl-1-propyl-1*H*-purine-2,6(3*H*,7*H*)-dione (**8c**)

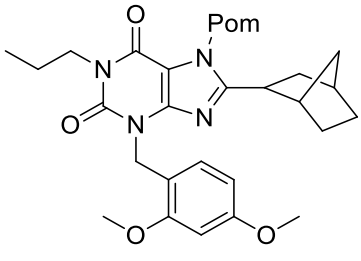

Beige crystals, 95%, mp 116 °C. ^{1}H-NMR (400 MHz, $CDCl_3$): δ 0.94 + 0.95 (2t, $^{3}J_{H\text{-}H}$ = 7.4 Hz, 3H, CH_3), 1.11 – 1.94 (m, 9H, N^{7}-Pom-CH_3, CH_3-CH_2, 2Nb-CH_2), 2.08 – 2.17 (m, 1H, C*H*), 2.34 – 2.43 (m, 2H, 2-Nb-CH_2), 2.82 – 2.86 (m, 0.4H), 3.25 – 3.30 (m, 0.6H), 3.78 (2s, 3H, 4-OCH_3), 3.83 (2s, 3H, 2-OCH_3), 3.96 – 4.00 (m, 2H, N^{1}-CH_2), 5.24 – 5.36 (m, 2H, Ph-CH_2), 6.13 – 6.31 (m, 2H, N^{7}-Pom-CH_2), 6.39 – 6.42 (m, 1H, Ph-*H*^{5}), 6.45 – 6.46 (m, 1H, Ph-*H*^{3}), 7.13 – 7.16 (m, 1H, Ph-*H*^{6}). ^{13}C-NMR (101 MHz, $CDCl_3$): δ 11.3, 21.3, 24.0, 26.9, 27.0, 28.8, 29.0, 29.7, 33.9, 36.0, 36.2, 36.3, 37.0, 38.1, 38.7, 38.8, 41.0, 41.4, 41.5, 42.4, 42.8, 43.2, 55.3, 55.4, 55.5, 66.6, 66.9, 98.4, 103.9, 104.0, 106.5, 107.0, 117.3, 117.4, 129.6, 129.7, 148.1, 148.3, 151.1, 151.2, 154.6, 154.8, 157.2, 158.3, 159.0, 160.2, 160.3, 177.2, 177.3. MS (ESI) calcd for $C_{30}H_{40}N_4O_6$, exact mass 552.29; m / z 553 $[M+H]^+$.

General procedure C: *N*-3 debenzylation, synthesis of xanthines 9a–c

Neat methanesulfonic acid (30 mL, 462 mmol) was added under argon at ambient temperature to a well stirred solution of the respective Pom-DMB-protected xanthine (**8a**-**c**) (10 mmol) and triethylsilane (3.2 mL, 20 mmol, 2 eq) in dry DCM (70 mL). When the reaction was complete (typically in less than one hour, TLC: ethyl acetate/hexane, 50/50, v/v), the mixture was poured into a stirred ice/sat. aqueous sodium bicarbonate mixture (500 mL) and stirring was continued for about 5 min. The mixture was transferred into a separatory funnel and extracted with diethyl ether (2 × 150 mL). The combined organic layers were washed with water (2 × 200 mL) and brine (200mL), dried over anhydrous Na_2SO_4, and concentrated under reduced pressure to afford the crude debenzylated xanthines as oils. Subsequent co-evaporation with methanol and cooling furnished solid residues, which were washed with hexane to remove a lipophilic yellow by-product (presumably 2,4-dimethoxytoluene). Finally, recrystallization of the nearly colorless solid materials thus obtained from aqueous methanol and drying at 80 °C afforded the desired xanthines (**9a–c**) as lightly colored solids.

8-(1-Norbornyl)-7-pivaloyloxymethyl-1-propyl-1*H*-purine-2,6(3*H*,7*H*)-dione (**9a**)

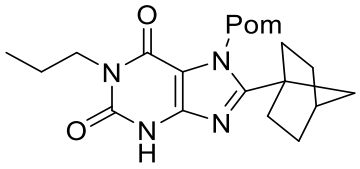

Tan powder, 78%, mp 219-220 °C. ^{1}H-NMR (400 MHz, DMSO-d_6): δ 0.85 (t, $^{3}J_{H\text{-}H}$ = 7.5 Hz, 3H, CH_3), 1.12 (s, 9H, N^{7}-Pom-CH_3), 1.29 – 1.93 (m, 12H, CH_3-CH_2 + 1-Nb-CH_2), 2.31 (s_{br}, 1H, 1-Nb-C*H*), 3.64 – 3.94 (m, 2H, N^{1}-CH_2), 6.23 (s, 2H, N^{7}-Pom-CH_2), 11.94 (s, 1H, N^{1}-*H*) . ^{13}C-NMR (101 MHz, DMSO-d_6): δ 11.5 (*C*H_3), 21.3 (CH_3-*C*H_2), 27.0 (N^{7}-Pom-*C*H_3), 30.3 (1-Nb-*C*H_2), 35.0 (1-Nb-*C*H_2), 36.4 (1-Nb-*C*H), 38.6 (N^{7}-Pom-*C*$(CH_3)_3$), 41.6 (1-Nb-*C*H_2), 43.5 (N^{1}-*C*H_2), 47.9 (1-Nb-*C*), 68.8 (N^{7}-Pom-*C*H_2), 106.6 (*C*^{5}), 147.2 (*C*^{4}), 151.1 (*C*^{2}), 155.0 (*C*^{6}), 159.1 (*C*^{8}), 176.6 (*C*=O). Elemental analysis calcd for $C_{21}H_{30}N_4O_4$: C 62.67, H 7.51, N 13.92; found: C 62.62, H 7.56, N 13.88. HRMS (ESI) *m*/*z* calcd for $C_{21}H_{30}N_4O_4$+H^+: 403.2340 [*M*+H]$^+$; found: 403.2338.

8-(7-Norbornyl)-7-pivaloyloxymethyl-1-propyl-1*H*-purine-2,6(3*H*,7*H*)-dione (**9b**)

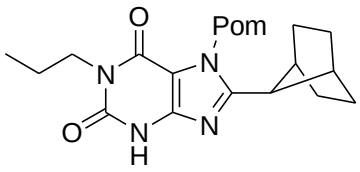

Light beige crystals, 80%, mp 218-219 °C. ^{1}H-NMR (400 MHz, DMSO-d_6): δ 0.86 (t, $^{3}J_{H-H}$ = 7.5 Hz, 3H, CH_3), 1.13 (s, 9H, N^{7}-Pom-CH_3), 1.19 – 1.41 (m, 4H, 7-Nb-CH_2), 1.43 – 1.64 (m, 2H, CH$_3$-CH_2), 1.66 – 1.92 (m, 4H, 7-Nb-CH_2), 2.51 (s_{br}, 2H, 7-Nb-C*H*), 3.05 (s_{br}, 1H, 7-Nb-C*H*), 3.69 – 3.94 (m, 2H, N^{1}-CH_2), 6.21 (s, 2H, N^{7}-Pom-CH_2), 11.92 (s, 1H, N^{3}-*H*). ^{13}C-NMR (101 MHz, DMSO-d_6): δ 11.6 (*C*H$_3$), 21.3 (CH$_3$-*C*H$_2$), 27.0 (N^{7}-Pom-*C*H$_3$), 28.1 (7-Nb-*C*H$_2$), 30.0 (7-Nb-*C*H$_2$), 38.7 (N^{7}-POM-*C*(CH$_3$)$_3$), 41.0 (7-Nb-*C*H), 41.6 (7-Nb-*C*H$_2$), 42.3 (N^{1}-*C*H$_2$), 46.3 (7-Nb-*C*H), 68.0 (N^{7}-Pom-*C*H$_2$), 106.0 (*C*^{5}), 147.3 (*C*^{4}), 151.1 (*C*^{2}), 154.9 (*C*^{6}), 155.6 (*C*^{8}), 176.7 (*C*=O). Elemental analysis calcd for $C_{21}H_{30}N_4O_4$: C 62.67, H 7.51, N 13.92; found: C 62.65, H 7.47, N 13.86. HRMS (ESI) *m*/*z* calcd for $C_{21}H_{30}N_4O_4$+H^{+}: 403.2340 [*M*+H]$^{+}$; found: 403.2343.

8-(2-*endo/exo*-Norbornyl)-7-pivaloyloxymethyl-1-propyl-1*H*-purine-2,6(3*H*,7*H*)-dione (**9c**)

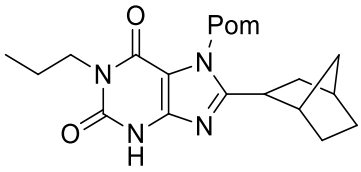

Colorless crystals, 82%, mp 176-177 °C. ^{1}H-NMR (400 MHz, DMSO-d_6): δ 0.97 (t, $^{3}J_{H-H}$ = 7.5 Hz, 3H, CH_3), 1.21 + 1.22 (2s, 9H, N^{7}-Pom-CH_3), 1.25 – 1.79 (m, 10H, CH$_3$-CH_2, 2-Nb-CH_2), 1.94 – 2.02 (m, 0.6H), 2.04 – 2.10 (m, 1H, C*H*), 2.39 – 2.50 (m, 2H), 2.87 – 2.91 (m, 0.3H), 3.30 – 3.36 (m, 0.7H), 3.96 – 4.00 (m, 2H, N^{1}-CH_2), 6.13 – 6.32 (m, 2H, N^{7}-Pom-CH_2), 9.13 + 9.19 (2s, 1H, N^{1}-*H*). ^{13}C-NMR (101 MHz, DMSO-d_6): δ 11.3, 21.3, 23.8, 26.9, 27.0, 27.2, 28.7, 29.3, 29.8, 33.6, 36.2, 36.3, 36.6, 37.0, 38.4, 38.8, 42.3, 42.4, 43.0, 55.7, 66.5, 66.8, 106.6, 107.0, 146.0, 146.1, 151.2, 154.8, 155.0, 157.8, 159.6, 177.2, 177.2. Elemental analysis calcd for $C_{30}H_{40}N_4O_6$: C 65.20, H 7.30, N 10.14; found: C 65.24, H 7.29, N 10.09. HRMS (ESI) *m*/*z* calcd for $C_{30}H_{40}N_4O_6$+H^{+}: 553.3021 [*M*+H]$^{+}$; found: 553.3024.

General procedure D: *N*-3 fluoropropylation, synthesis of xanthines 10a–c

Dry potassium carbonate (1.52 g, 11 mmol) was added under argon at 60 °C to a stirred suspension of the respective xanthine (**9a**-**c**) (10 mmol) in dry DMF (100 mL). The mixture was stirred for 30 min, 3-fluoropropylmesylate (MW 156.18, $d_{calc.}$ 1.225, 1.66 mL, 13 mmol) was added, and the mixture was stirred at 60 °C for another 2 h (TLC: ethyl acetate/hexane, 50/50, v/v). After cooling to ambient temperature, the reaction mixture was poured into a stirred ice/water mixture (500 mL) and the resulting semi-solid precipitate was extracted into diethyl ether (3 × 100 mL). The combined organic layers were washed with water (2 × 150 mL), dried over anhydrous Na_2SO_4, and concentrated under reduced pressure to afford the desired xanthines as a solid (**10b**) or yellow oils (pure by TLC) that solidified upon standing (**10a** and **10c**). The solid products were recrystallized from aqueous methanol.

3-(3-Fluoropropyl)-8-(1-norbornyl)-7-pivaloyloxymethyl-1-propyl-1*H*-purine-2,6(3*H*,7*H*)-dione (**10a**)

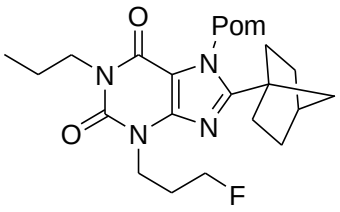

Colorless crystals, 76%, mp 120-121 °C. ^{1}H-NMR (400 MHz, $CDCl_3$): δ 0.96 (t, $^{3}J_{H\text{-}H}$ = 7.5 Hz, 3H, CH_3), 1.21 (s, 9H, N^7-POM-CH_3), 1.38 – 1.97 (m, 12H, CH_3-CH_2 + 1-Nb-CH_2), 2.22 (dm, *J* = 27.3, 6.1 Hz, 2H, CH_2-CH_2F), 2.41 (s_{br}, 1H, 1-Nb-C*H*), 3.91 – 4.06 (m, 2H, N^1-CH_2), 4.28 (t, $^{3}J_{H\text{-}H}$ = 6.7 Hz, 2H, N^3-CH_2), 4.58 (dt, $^{2}J_{H\text{-}F}$ = 47.2 Hz, $^{3}J_{H\text{-}H}$ 5,7 Hz, 2H, CH_2-F), 6.30 (s, 2H, N^7-Pom-CH_2). ^{13}C-NMR (101 MHz, $CDCl_3$): δ 11.3 (*C*H_3), 21.3 (CH_3-*C*H_2), 27.0 (N^7-Pom-*C*H_3), 29.4 ($^{2}J_{C\text{-}F}$ = 19.2 Hz, *C*H_2-CH_2F), 30.4 (1-Nb-*C*H_2), 35.2 (1-Nb-*C*H_2), 36.4 (1-Nb-*C*H), 38.8 (N^7-Pom-*C*(CH_3)$_3$), 40.0 ($^{3}J_{C\text{-}F}$ = 5.5 Hz, N^3-*C*H_2), 42.8 (1-Nb-*C*H_2), 43.5 (N^1-*C*H_2), 47.9 (1-Nb-*C*^{1}), 68.5 (N^7-POM-*C*H_2), 82.0 ($^{1}J_{C\text{-}F}$ = 162.0 Hz, *C*H_2F), 107.2 (*C*^{5}), 147.54 (*C*^{4}), 151.2 (*C*^{2}), 154.4 (*C*^{6}), 158.9 (*C*^{8}), 177.1 (*C*=O). ^{19}F-NMR (376 MHz, $CDCl_3$): δ - 219.97. Elemental analysis calcd for $C_{24}H_{35}FN_4O_4$: C 62.32, H 7.63, N 12.11; found: C 62.30, H 7.59, N 12.18. HRMS (ESI) *m*/*z* calcd for $C_{24}H_{35}FN_4O_4$+H^+: 463.2715 [*M*+H]$^+$; found: 463.2711.

3-(3-Fluoropropyl)-8-(7-norbornyl)-7-pivaloyloxymethyl-1-propyl-1*H*-purine-2,6(3*H*,7*H*)-dione (10b)

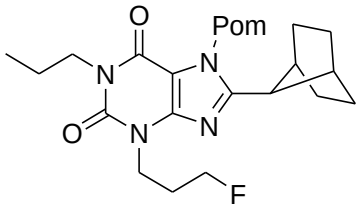

Off white crystals, 83%, mp 166-167 °C. ^{1}H-NMR (400 MHz, $CDCl_3$): δ 0.96 (t, $^{3}J_{H\text{-}H}$ = 7.5 Hz, 3H, CH_3), 1.22 (s, 9H, N^7-Pom-CH_3), 1.28 – 1.43 (m, 4H, 7-Nb-CH_2), 1.66 – 1.72 (m, 2H, CH_3-CH_2), 1.76 – 1.97 (m, 4H, 7-Nb-CH_2), 2.13 – 2.26 (m, 2H, CH_2-CH_2F), 2.56 (s_{br}, 2H, 7-Nb-C*H*), 2.87 (s_{br}, 1H, 7-Nb-C*H*), 3.96 – 3.99 (m, 2H, N^1-CH_2), 4.27 (t, $^{3}J_{H\text{-}H}$ = 6.7 Hz, 2H, N^3-CH_2), 4.56 (dt, $^{2}J_{H\text{-}F}$ = 47.2 Hz, $^{3}J_{H\text{-}H}$ 5,7 Hz, 2H, CH_2-F), 6.26 (s, 2H, N^7-Pom-CH_2). ^{13}C-NMR (101 MHz, $CDCl_3$): δ 11.3 (*C*H_3), 21.3 (CH_3-*C*H_2), 27.0 (N^7-Pom-*C*H_3), 28.1 (7-Nb-*C*H_2), 29.3 ($^{2}J_{C\text{-}F}$ = 19.2 Hz, *C*H_2-CH_2F), 30.1 (7-Nb-*C*H_2), 38.9 (N^7-Pom-*C*(CH_3)$_3$), 40.0 ($^{3}J_{C\text{-}F}$ = 5.5 Hz, N^3-*C*H_2), 41.4 (7-Nb-*C*H), 42.5 (N^1-*C*H_2), 42.9 (7-Nb-*C*H_2), 46.4 (7-Nb-*C*H), 67.2 (N^7-Pom-*C*H_2), 81.9 ($^{1}J_{C\text{-}F}$ = 162.0 Hz , *C*H_2F), 106.5 (*C*^{5}), 147.8 (*C*^{4}), 151.2 (*C*^{2}), 154.5 (*C*^{6}), 155.2 (*C*^{8}), 177.2 (*C*=O). ^{19}F-NMR (376 MHz, $CDCl_3$): δ - 219.98. Elemental analysis calcd for $C_{24}H_{35}FN_4O_4$: C 62.32, H 7.63, N 12.11; found: C 62.34, H 7.62, N 12.07. HRMS (ESI) *m*/*z* calcd for $C_{24}H_{35}FN_4O_4$+H^+: 463.2715 [*M*+H]$^+$; found: 463.2714.

3-(3-Fluoropropyl)-8-(2-*endo/exo*-norbornyl)-7-pivaloyloxymethyl-1-propyl-1*H*-purine-2,6(3*H*,7*H*)-dione (10c)

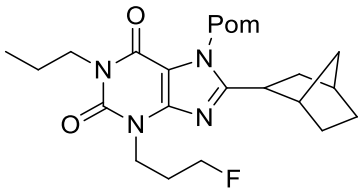

Tan crystals, 86%, mp 96 °C. ^{1}H-NMR (400 MHz, $CDCl_3$) δ 0.95 (t, $^{3}J_{H\text{-}H}$ 7.4 Hz, 3H, C*H*$_3$-CH$_2$), 1.19 + 1.20 (2s, 9H, N^{7}-Pom-C*H*$_3$), 1.26 – 1.96 (m, 8H, CH$_3$-C*H*$_2$, 2-Nb-C*H*$_2$), 2.10 – 2.27 (m, 3H, C*H*, C*H*$_2$-C*H*$_2$F), 2.34 – 2.45 (t, $^{3}J_{H\text{-}H}$ 4.4 Hz, 1H, C$^{4'}$*H*), 2.89 (s_{br}, 1H, C$^{1'}$*H*), 3.33 (s_{br}, 1H, C$^{2'}$*H*), 4.02 (t, 2H, $^{3}J_{H\text{-}H}$ 6.7 Hz N^{1}-C*H*$_2$), 4.32 (m, 2H), 2.81 – 2.87 (m, 0.3H), 3.26 – 3.33 (m, 0.6H), 3.95 – 3.98 (m, 2H,), 4.24 – 4.30 (m, 2H), 4.48 – 4.51 (m, 1H, 0.5 CH$_2$-C*H*$_2$-F), 4.59 – 4.63 (m, 1H, 0.5 CH$_2$-C*H*$_2$-F), 6.11 – 6.30 (m, 2H, N^{7}-Pom-C*H*$_2$). ^{13}C-NMR (101 MHz, $CDCl_3$) δ 11.3, 21.3, 24.1, 26.9, 27.0, 28.7, 29.0, 29.2, 29.4, 29.4, 29.8, 33.9, 36.0, 36.2, 36.4, 37.0, 38.1, 38.7, 38.8, 39.9, 39.9, 40.0, 40.0, 40.9, 42.5, 42.8, 43.2, 81.0, 81.1, 82.6, 82.7, 106.6, 107.0, 147.6, 147.7, 151.2, 154.4, 154.6, 157.5, 159.3, 177.2, 177.2. ^{19}F-NMR (376 MHz, $CDCl_3$): δ - 219.9, - 220.0. Elemental analysis calcd for $C_{24}H_{35}FN_4O_4$: C 62.32, H 7.63, N 12.11; found: C 62.30, H 7.66, N 12.14. HRMS (ESI) *m*/*z* calcd for $C_{24}H_{35}FN_4O_4$+H^{+}: 463.2715 [*M*+H]$^{+}$; found: 463.2719.

General procedure E: *N*-7 deprotection, synthesis of xanthines 11a–c

Aqueous 1 N NaOH (2 mL, 2 mmol, 2 equiv) was added at ambient temperature to a stirred mixture of the respective Pom-protected intermediates (**10a**-**c**) (1 mmol) in methanol (2 mL). After 10 min, a clear solution had formed (TLC: 2% acetic acid in ethyl acetate/hexane, 50/50, v/v), which was neutralized by addition of aqueous 1 N HCl (2 mL, 2 mmol) and diluted with water (10 mL). The deprotected xanthines were collected by filtration, washed with water, and dried at 100 °C.

3-(3-Fluoropropyl)-8-(1-norbornyl)-1-propyl-1*H*-purine-2,6(3*H*,7*H*)-dione (**11a, 1-NBX**)

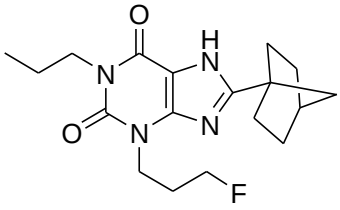

Colorless crystals, 82%, mp 173 °C. ^{1}H-NMR (400 MHz, DMSO-*d*$_6$): δ 0.87 (t, $^{3}J_{H\text{-}H}$ = 7.5 Hz, 3H, C*H*$_3$), 1.27 – 2.24 (m, 14H, CH$_3$-C*H*$_2$ + 1-Nb-C*H*$_2$ + C*H*$_2$-CH$_2$F), 2.34 (s_{br}, 1H, 1-Nb-C*H*), 3.78 – 3.92 (m, 2H, N^{1}-C*H*$_2$), 4.11 (t, *J* = 6.7 Hz, 2H, N^{3}-C*H*$_2$), 4.52 (dt, $^{2}J_{H\text{-}F}$ = 47.2 Hz, $^{3}J_{H\text{-}H}$ 5,7 Hz, 2H, C*H*$_2$-F), 13.09 (s_{br}, 1H, N^{7}-*H*). ^{13}C-NMR (101 MHz, DMSO-*d*$_6$): δ 11.6 (*C*H$_3$), 21.3 (CH$_3$-*C*H$_2$), 29.2 ($^{2}J_{C\text{-}F}$ = 19.2 Hz, *C*H$_2$-CH$_2$F), 30.3 (1-Nb-*C*H$_2$), 34.9 (1-Nb-*C*H$_2$), 37.7 (1-Nb-*C*H), 40.1 ($^{3}J_{C\text{-}F}$ = 5.5 Hz, N^{3}-*C*H$_2$), 42.5 (1-Nb-*C*H$_2$), 43.8 (N^{1}-*C*H$_2$), 47.6 (1-Nb-*C*^{1}), 82.4 ($^{1}J_{C\text{-}F}$ = 162.0 Hz, *C*H$_2$F), 107.0 (*C*^{5}), 147.9 (*C*^{4}), 151.2 (*C*^{2}), 154.3 (*C*^{6}), 158.0 (*C*^{8}). ^{19}F-NMR (376 MHz, DMSO-*d*$_6$): δ - 218.36. MS (ESI) calcd for $C_{18}H_{25}FN_4O_2$, exact mass 348.20; m / z 349 [M+H]$^{+}$. Elemental analysis calcd for $C_{24}H_{35}FN_4O_4$: C 62.32, H 7.63, N 12.11; found: C 62.30, H 7.59, N 12.18. HRMS (ESI) *m*/*z* calcd for $C_{24}H_{35}FN_4O_4$+H^{+}: 463.2715 [*M*+H]$^{+}$; found: 463.2711.

3-(3-Fluoropropyl)-8-(7-norbornyl)-1-propyl-1*H*-purine-2,6(3*H*,7*H*)-dione (**11b, 7-NBX**)

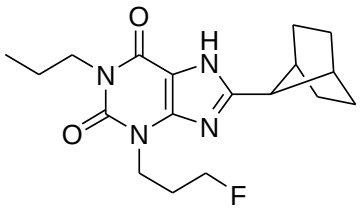

Colorless crystals, 89%, mp 168 °C. ^{1}H-NMR (400 MHz, DMSO-d_6): δ 0.88 (t, $^{3}J_{H\text{-}H}$ = 7.5 Hz, 3H, CH_3), 1.09 – 1.39 (m, 4H, 7-Nb-CH_2), 1.46 – 1.81 (m, 6H, 7-Nb-CH_2 + CH$_3$-CH_2), 2.07 (dt, $^{3}J_{H\text{-}F}$ = 27.3 Hz, $^{3}J_{H\text{-}H}$ 6.1 Hz, 2H, CH_2-CH$_2$F), 2.67 (s_{br}, 2H, 7-Nb-CH), 2.83 (s_{br}, 1H, 7-Nb-CH), 3.75 – 3.91 (m, 2H, N^1-CH_2), 4.12 (t, $^{3}J_{H\text{-}H}$ = 6.7 Hz, 2H, N^3-CH_2), 4.49 (dt, $^{2}J_{H\text{-}F}$ = 47.2 Hz, $^{3}J_{H\text{-}H}$ 5,7 Hz, 2H, CH_2-F), 13.09 (s_{br}, 1H, N^7-H). ^{13}C-NMR (101 MHz, DMSO-d_6): δ 11.6 (*C*H$_3$), 21.31 (CH$_3$-*C*H$_2$), 28.0 (7-Nb-*C*H$_2$), 29.3 ($^{2}J_{C\text{-}F}$ = 19.2 Hz, *C*H$_2$-CH$_2$F), 30.0 (7-Nb-*C*H$_2$), 39.9 ($^{3}J_{C\text{-}F}$ = 5.5 Hz, N^3-*C*H$_2$), 40.0 (7-Nb-*C*H), 42.5 (7-Nb-*C*H$_2$), 43.0 (N^1-*C*H$_2$), 48.6 (7-Nb-*C*H), 82.3 ($^{1}J_{C\text{-}F}$ = 162.0 Hz , *C*H$_2$F), 106.7 (*C*^{5}), 148.0 (*C*^{4}), 151.1 (*C*^{2}), 154.3 (*C*^{6}), 155.4 (*C*^{8}). ^{19}F-NMR (376 MHz, DMSO-d_6): δ - 218.34. Elemental analysis calcd for $C_{24}H_{35}FN_4O_4$: C 62.32, H 7.63, N 12.11; found: C 62.31, H 7.65, N 12.16. HRMS (ESI) *m*/*z* calcd for $C_{24}H_{35}FN_4O_4$+H$^+$: 463.2715 [*M*+H]$^+$; found: 463.2714.

3-(3-Fluoropropyl)-8-(2-*endo/exo*-norbornyl)-1-propyl-1*H*-purine-2,6(3*H*,7*H*)-dione (**11c, 2-NBX**)

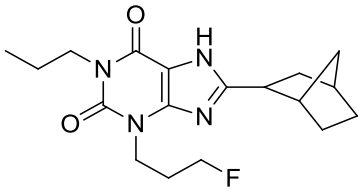

Colorless crystals, 92%, mp 170 °C. ^{1}H-NMR (400 MHz, CDCl$_3$) δ 1.05 (t, $^{3}J_{H\text{-}H}$ 7.3 Hz, 3H, CH_3-CH$_2$), 1.14–1.92 (m, 8H, CH$_3$-CH_2, C$^{5'}H_2$, C$^{6'}H_2$, C$^{7'}H_2$), 2.07 (m, 2H, C$^{3'}H_2$), 2.28 (dt, $^{3}J_{H\text{-}F}$ = 25.6 Hz, $^{3}J_{H\text{-}H}$ 5.9 Hz, 2H, CH_2-CH$_2$F), 2.34 (t, $^{3}J_{H\text{-}H}$ 4.4 Hz, 1H, C$^{4'}H$), 2.81 (s_{br}, 1H, C$^{1'}H$), 3.40 (s_{br}, 1H, C$^{2'}H$), 4.1 (t, 2H, $^{3}J_{H\text{-}H}$ 7.3 Hz N^1-CH_2), 4.39 (m, 2H, N^3-CH_2), 4.62 (dt, $^{2}J_{H\text{-}F}$ = 47.2 Hz, $^{3}J_{H\text{-}H}$ 5,6 Hz, 2H, CH$_2$-CH_2-F), 12.70 (s_{br}, 1H, N^7*H*). ^{13}C-NMR (101 MHz, CDCl$_3$) δ 11.4 (*C*H$_3$-CH$_2$), 21.4 (CH$_3$-*C*H$_2$), 24.2 (C$^{6'}$), 29.2 ($^{3}J_{C\text{-}F}$ = 19.6 Hz, *C*H$_2$-CH$_2$F), 29.4 (C$^{5'}$), 37.27 (C$^{4'}$), 40.3 (*J* = 5.5 Hz, N^3-*C*H$_2$), 40.3 (C$^{7'}$), 40.9 (C$^{1'}$), 41.5 (C$^{3'}$), 42.5 (C$^{2'}$), 43.5 (N^1-*C*H$_2$), 82.1 ($^{1}J_{C\text{-}F}$ = 162.0 Hz , *C*H$_2$F), 106.9 (*C*^{5}), 148.4 (*C*^{4}), 151.0 (*C*^{2}), 155.5 (*C*^{6}), 158.0 (*C*^{8}). ^{19}F-NMR (376 MHz, CDCl$_3$): δ - 219.8. Elemental analysis calcd for $C_{24}H_{35}FN_4O_4$: C 62.32, H 7.63, N 12.11; found: C 62.36, H 7.60, N 12.07. HRMS (ESI) *m*/*z* calcd for $C_{24}H_{35}FN_4O_4$+H$^+$: 463.2715 [*M*+H]$^+$; found: 463.2711.

3-(3-Hydroxypropyl)-8-(1-norbornyl)-7-pivaloyloxymethyl-1-propyl-1*H*-purine-2,6(3*H*,7*H*)-dione (12a)

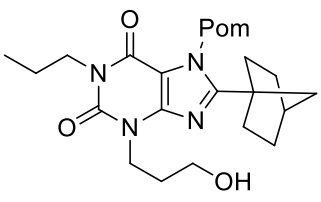

12a was prepared according to **general procedure D** using 8-(1-norbornyl)-7-pivaloyloxymethyl-1-propyl-1*H*-purine-2,6(3*H*,7*H*)-dione (**9a**) (2 g, 5 mmol), dry potassium carbonate (760 mg, 5.5 mmol) and 3-bromo-1-propanol (903 mg, 588 µL, 6.5 mmol). Work-up afforded the title compound (1.93g, 4.3 mmol, 86%) as a colorless oil that turned into a low-melting, colorless waxy solid upon standing, mp 57-58 °C. ^{1}H-NMR (400 MHz, $CDCl_3$): δ 0.96 (t, $^{3}J_{H\text{-}H}$ = 7.4 Hz, 3H, C*H*$_3$), 1.22 (s, 9H, N^7-Pom-C*H*$_3$), 1.37 – 2.05 (m, 14H, CH_3-C*H*$_2$ + N^3-CH_2-C*H*$_2$ + 1-Nb-C*H*$_2$), 2.43 (s_{br}, 1H, 1-Nb-C*H*), 3.49-3.56 (m, 2H, C*H*$_2$OH), 3.71 - 3.84 (m, 1H, O*H*), 3.94 – 4.01 (m, 2H, N^1-C*H*$_2$), 4.24 – 4.30 (m, 2H, N^3-C*H*$_2$), 6.30 (s, 2H, N^7-Pom-C*H*$_2$). ^{13}C-NMR (101 MHz, $CDCl_3$): δ 11.3 (*C*H_3), 21.3 (CH_3-*C*H_2), 26.9 (N^7-Pom-*C*H_3), 30.3 (1-Nb-*C*H_2), 31.1 (N^3-CH_2-*C*H_2), 35.2 (1-Nb-*C*H_2), 36.4 (1-Nb-*C*H), 38.8 (N^7-Pom-*C*$(CH_3)_3$), 39.5 (N^3-*C*H_2), 42.9 (1-Nb-*C*H_2), 43.5 (N^1-*C*H_2), 47.8 (1-Nb-*C*^{1}), 57.6 (*C*H_2OH), 68.5 (N^7-Pom-*C*H_2), 106.9 (*C*^{5}), 147.8 (*C*^{4}), 151.3 (*C*^{2}), 154.3 (*C*^{6}), 158.9 (*C*^{8}), 177.1 (*C*=O). Elemental analysis calcd for $C_{24}H_{36}N_4O_5$: C 62.59, H 7.88, N 12.16; found: C 62.54, H 7.92, N 12.19. HRMS (ESI) *m*/*z* calcd for $C_{24}H_{36}N_4O_5$+H^+: 461.2758 [*M*+H]$^+$; found: 461.2761.

3-(3-Toluenesulfonylpropyl)-8-(1-norbornyl)-7-pivaloyloxymethyl-1-propyl-1*H*-purine-2,6(3*H*,7*H*)-dione (13a)

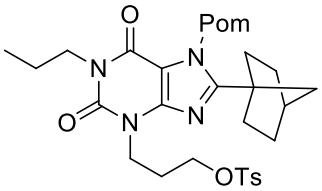

Under an argon atmosphere, a stirred solution of alcohol **11a** (920 mg, 2 mmol) in anhydrous acetonitrile (12 mL) was cooled to 0 °C using an ice/NaCl-bath. After the addition of 1,6-bis(dimethylamino)hexane (639 µL, 4.6 mmol), a solution of *p*-toluenesulfonic acid (382 mg, 2 mmol) in anhydrous acetonitrile (6 mL) was added dropwise. The reaction mixture was stirred at 0 °C for 60 min and at ambient temperature for another 4 h. *N,N*'-Dimethylpropane-1,3-diamine (245 µL, 2 mmol) was then added and the mixture was stirred for 15 min, after which water (50 mL) was added and the aqueous mixture extracted with DCM (2 × 50 mL). The combined organic layers were washed with water (50 mL) and brine (50 mL) and dried over anhydrous Na_2SO_4. The solvent was removed under reduced pressure and the residue was purified by column chromatography (silica gel; ethyl acetate/hexane, 50/50, v/v) to afford the title compound (1 g, 1.64 mmol, 82%) as colorless crystals, mp 135 °C. ^{1}H-NMR (400 MHz, $CDCl_3$): δ 0.94 (t, $^{3}J_{H\text{-}H}$ = 7.5 Hz, 3H, C*H*$_3$), 1.21 (s, 9H, N^7-Pom-C*H*$_3$), 1.45 – 1.54 (m, 2H, 1-Nb-C*H*$_2$), 1.62 (sx, $^{3}J_{H\text{-}H}$ = 7.5 Hz, 2H, CH_3-C*H*$_2$), 1.77-1.88 (m, 6H, 1-Nb-C*H*$_2$), 1.90 (s_{br}, 2H, 1-Nb-C*H*$_2$), 2.17 (p, $^{3}J_{H\text{-}H}$ = 6.6 Hz, 2H, N^3-CH_2-C*H*$_2$), 2.40 (s_{br}, 1H, 1-Nb-C*H*), 2.46 (s, 3H, aryl-C*H*$_3$), 3.90 – 3.95 (m, 2H, N^1-C*H*$_2$), 4.13-4.19 (m, 4H, N^3-C*H*$_2$ + C*H*$_2$OTs), 6.28 (s, 2H, N^7-Pom-C*H*$_2$) 7.34 (d, $^{3}J_{H\text{-}H}$ = 8 Hz, aryl-*H*^{3}), 7.78 (d, $^{3}J_{H\text{-}H}$ = 8.3 Hz, aryl-*H*^{2}). ^{13}C-NMR (101 MHz, $CDCl_3$): δ 11.3 (*C*H_3), 21.2 (CH_3-*C*H_2), 21.7 (aryl-*C*H_3), 26.9 (N^7-Pom-*C*H_3), 27.8 (N^3-CH_2-*C*H_2), 30.4 (1-Nb-*C*H_2), 35.2 (1-Nb-*C*H_2), 36.3 (1-Nb-*C*H), 38.8 (N^7-Pom-*C*$(CH_3)_3$), 40.1 (N^3-*C*H_2), 42.8 (1-Nb-*C*H_2), 43.9 (N^1-*C*H_2), 47.9 (1-Nb-*C*^{1}), 68.1 (*C*H_2-

OTs), 68.5 (N^7-POM-CH_2), 107.2 (C^5), 127.8 (aryl-C^2), 129.9 (aryl-C^3), 133.0 (aryl-C^4), 144.8 (aryl-C^1), 147.4 (C^4), 151.1 (C^2), 154.3 (C^6), 159.0 (C^8), 177.1 (*C*=O). Elemental analysis calcd for $C_{31}H_{42}N_4O_7S$: C 60.57, H 6.89, N 9.11; found: C 62.59, H 6.94, N 9.19. HRMS (ESI) *m/z* calcd for $C_{31}H_{42}N_4O_7S+H^+$: 615.2846 $[M+H]^+$; found: 615.2849.

3-(2-(2-Hydroxyethoxy)ethyl)-8-(1-norbornyl)-7-pivaloyloxymethyl-1-propyl-1*H*-purine-2,6(3*H*,7*H*)-dione (14)

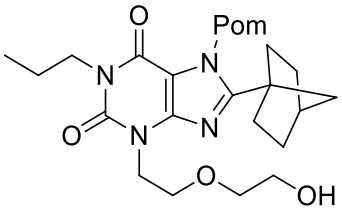

14 was prepared according to **general procedure D** using 8-(1-norbornyl)-7-pivaloyloxymethyl-1-propyl-1*H*-purine-2,6(3*H*,7*H*)-dione (**9a**) (4 g, 10 mmol), dry potassium carbonate (1420 mg, 11 mmol) and 2-(2-chloroethoxy)-ethanol (1620 mg, 1380 µL, 13 mmol). Work-up and purification by FC (silica gel, ethyl acetate/methanol, 90/10, v/v) afforded the title compound (3.33 g, 6.6 mmol, 66%) as a colorless oil that solidified into a yellow waxy solid upon standing, mp 110-111 °C. ^{1}H-NMR (400 MHz, $CDCl_3$): δ 0.95 (t, $^3J_{H-H}$ = 7.4 Hz, 3H, C*H*$_3$), 1.21 (s, 9H, N^7-Pom-C*H*$_3$), 1.43 – 1.55 (m, 2H, 1-Nb-C*H*$_2$), 1.66 (sx, 2H, $^3J_{H-H}$ = 7.4 Hz, CH_3-C*H*$_2$), 1.74 – 1.87 (m, 6H, 1-Nb-C*H*$_2$) 1.90 (s_{br}, 2H, 1-Nb-C*H*$_2$) 2.39 (s_{br}, 1H, 1-Nb-C*H*), 2.82 (s_{br}, 1H, O-CH_2-CH_2O*H*), 3.66 - 3.71 (m, 4H, O-C*H*$_2$-C*H*$_2$OH), 3.91 (t, 2H, $^3J_{H-H}$ = 5.2 Hz, N^1-C*H*$_2$), 3.94 – 3.98 (m, 2H, N^3-C*H*$_2$), 4.33 (t, 2H, $^3J_{H-H}$ = 5.2 Hz, N^3-CH_2 –C*H*$_2$), 6.29 (s, 2H, N^7-Pom-C*H*$_2$). ^{13}C-NMR (101 MHz, $CDCl_3$): δ 11.3 (*C*H$_3$), 21.3 (CH_3-*C*H$_2$), 26.9 (N^7-Pom-*C*H$_3$), 30.3 (1-Nb-*C*H$_2$), 35.2 (1-Nb-*C*H$_2$), 36.4 (1-Nb-*C*H), 38.8 (N^7-Pom-*C*(CH_3)$_3$), 42.9 (N^3-*C*H_2-CH_2), 43.1 (1-Nb-*C*H$_2$), 43.5 (N^1-*C*H$_2$), 47.9 (1-Nb-*C*^{1}), 61.7 (O-CH_2-*C*H_2OH), 68.5 (N^7-Pom-*C*H$_2$), 68.7 (N^3-CH_2-*C*H$_2$), 72.8 (O-*C*H_2-CH_2OH), 106.9 (C^5), 147.8 (C^4), 151.3 (C^2), 154.3 (C^6), 158.9 (C^8), 177.1 (*C*=O). Elemental analysis calcd for $C_{25}H_{38}N_4O_6$: C 61.21, H 7.81, N 11.42; found: C 61.54, H 7.78, N 11.19. HRMS (ESI) *m/z* calcd for $C_{25}H_{38}N_4O_6+H^+$: 491.2864 $[M+H]^+$; found: 491.2831.

3-(2-(2-((Methylsulfonyl)oxy)ethoxy)ethyl)-8-(1-norbornyl)-7-pivaloyloxymethyl-1-propyl-1*H*-purine-2,6(3*H*,7*H*)-dione (15)

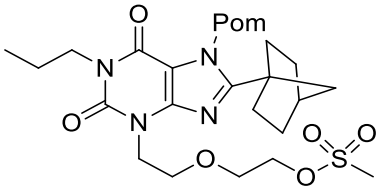

Under an argon atmosphere, a stirred solution of alcohol **14** (2.45 g, 5 mmol) in dry DCM (20 mL) was cooled to 0 °C using an ice/NaCl-bath. After the addition of triethylamine (1050 µL, 7.5 mmol), methanesulfonyl chloride (430 µL, 5.5 mmol) was added dropwise. The reaction mixture was stirred at 0 °C for 1 h and at ambient temperature for another 1 h. More DCM (50 mL) was then added and the

organic solution was washed with water (2 × 50 mL), sat. aqueous $NaHCO_3$ solution (50 mL) and brine (50 mL). The organic layer was separated and dried over anhydrous Na_2SO_4. Evaporation of the solvent under reduced pressure afforded the title compound (2.56 g, 4.4 mmol, 88%) as a yellow oil. Due to limited stability, **15** was directly used for the next step without further purification.

3-(2-(2-Fluoroethoxy)ethyl)-8-(1-norbornyl)-7-pivaloyloxymethyl-1-propyl-1*H*-purine-2,6(3*H*,7*H*)-dione (16)

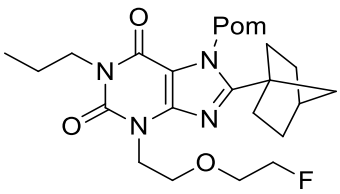

Under an argon atmosphere, mesylate **15** (2.27 g, 4 mmol) was dissolved in warm (30-40 °C) *tert*-butanol (20 mL). Under efficient stirring, CsF (1.82 g, 12 mmol) was added and the reaction mixture was stirred at 80 °C for 6 h. After cooling to ambient temperature, diethyl ether (100 mL) was added and insoluble material was removed by filtration. The filtrate was concentrated under reduced pressure and the residue purified by FC (silica gel, ethyl acetate/hexane, 70/30, v/v) to afford the title compound (1.5 g, 2.96 mmol, 74%) as an oil, which solidified into colorless crystals upon standing, mp 93 °C. ^{1}H-NMR (400 MHz, DMSO-d_6): δ 0.95 (t, $^3J_{H\text{-}H}$ = 7.4 Hz, 3H, CH_3), 1.20 (s, 9H, N^7-Pom-CH_3), 1.43 – 1.54 (m, 2H, 1-Nb-CH_2), 1.67 (sx, 2H, $^3J_{H\text{-}H}$ = 7.4 Hz, CH_3-CH_2), 1.75 – 1.86 (m, 6H, 1-Nb-CH_2) 1.87 (s_{br}, 2H, 1-Nb-CH_2) 2.38 (s_{br}, 1H, 1-Nb-C*H*), 3.84 - 3.68 (dt, 2H, *J* = 29.5, 4.2 Hz, O-CH_2-CH_2-F), 3.89 – 3.98 (m, 4H, N^1-CH_2 + N^3-CH^2-CH^2), 4.33 (t, 2H, $^3J_{H\text{-}H}$ = 5.8 Hz, N^3-CH_2), 4.52 (t, 2H, *J* = 47.7, 4.2 Hz, O-CH_2-CH_2-F). ^{13}C-NMR (101 MHz, DMSO-d_6): δ 11.3 (*C*H_3), 21.3 (CH_3-*C*H_2), 26.9 (N^7-Pom-*C*H_3), 30.4 (1-Nb-*C*H_2), 35.2 (1-Nb-*C*H_2), 36.3 (1-Nb-*C*H), 38.7 (N^7-Pom-*C*$(CH_3)_3$), 41.6 (N^3-*C*H_2-CH_2), 42.8 (1-Nb-*C*H_2), 43.6 (N^1-*C*H_2), 47.9 (1-Nb-*C*^{1}), 68.0 (N^7-Pom-*C*H_2), 68.5 (N^3-CH_2-*C*H_2), 69.4 (d, *J* = 19.8 Hz, O-*C*H_2-CH_2-F), 83.2 (d, *J* = 170.2 Hz, O-CH_2-*C*H_2-F), 107.2 (*C*^{5}), 148.7 (*C*^{4}), 151.3 (*C*^{2}), 154.4 (*C*^{6}), 158.7 (*C*^{8}), 177.1 (*C*=O). ^{19}F-NMR (376 MHz, DMSO-d_6): δ 223.7. Elemental analysis calcd for $C_{25}H_{37}FN_4O_5$: C 60.96, H 7.57, N 11.37; found: C 61.04, H 7.51, N 11.36. HRMS (ESI) *m/z* calcd for $C_{25}H_{37}FN_4O_5$+H^+: 493.2821 $[M+H]^+$; found: 493.2819.

3-(2-(2-Fluoroethoxy)ethyl)-8-(1-norbornyl)-1-propyl-1*H*-purine-2,6(3*H*,7*H*)-dione (17, 1-NBXOF)

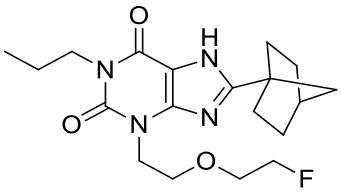

17 was prepared according to **general procedure E** using 3-(2-(2-fluoroethoxy)ethyl)-8-(1-norbornyl)-7-pivaloyloxymethyl-1-propyl-1*H*-purine-2,6(3*H*,7*H*)-dione (**16**) (493 mg, 1 mmol), which afforded the title compound (369 mg, 0.94 mmol, 94%) as a colorless solid, mp 131-132 °C. ^{1}H-NMR (400 MHz, DMSO-d_6): δ 0.87 (t, $^3J_{H\text{-}H}$ = 7.4 Hz, 3H, CH_3), 1.32 – 1.42 (m, 2H, 1-Nb-CH_2), 1.56 (sx, 2H, $^3J_{H\text{-}H}$ = 7.4 Hz,

CH_3-CH_2), 1.62 – 1.76 (m, 6H, 1-Nb-CH_2) 1.86 – 1.97 (m, 2H, 1-Nb-CH_2) 2.30 – 2.37 (m, 1H, 1-Nb-C*H*), 3.64 – 3.68 (m, 1H, 0.5 O-CH_2-CH_2-F), 3.71 - 3.77 (m, 3H, 0.5 O-CH_2-CH_2-F + N^1-CH_2), 3.81 – 3.87 (m, 2H, N^3-CH_2), 4.16 (t, 2H, $^3J_{H\text{-}H}$ = 6.2 Hz, N^3-CH_2 –CH_2), 4.45 (dt, 2H, *J* = 47.9, 4.0 Hz, O-CH_2-CH_2-F), 13.09 (s, 1H, N^7-*H*). ^{13}C-NMR (101 MHz, DMSO-d_6): δ 11.6 (*C*H_3), 21.3 (CH_3-*C*H_2), 30.3 (1-Nb-*C*H_2), 34.9 (1-Nb-*C*H_2), 37.7 (1-Nb-*C*H), 42.2 (N^3-*C*H_2-CH_2), 42.5 (1-Nb-*C*H_2), 43.7 (N^1-*C*H_2), 47.6 (1-Nb-*C*^{1}), 67.2 (N^3-CH_2-*C*H_2), 69.6 (d, *J* = 18.8 Hz, O-*C*H_2-CH_2-F), 83.4 (d, *J* = 166 Hz, O-CH_2-*C*H_2-F) 106.9 (*C*^{5}), 148.1 (*C*^{4}), 151.2 (*C*^{2}), 154.3 (*C*^{6}), 158.0 (*C*^{8}). ^{19}F-NMR (376 MHz, DMSO-d_6): δ 221.9. Elemental analysis calcd for $C_{19}H_{27}FN_4O_3$: C 60.30, H 7.19, N 14.80; found: C 60.34, H 7.28, N 14.99. HRMS (ESI) *m/z* calcd for $C_{19}H_{27}FN_4O_3$+H^+: 379.2139 $[M+H]^+$; found: 379.2143.

4.6. Radiochemistry

General

[^{18}F]Fluoride was produced via the ^{18}O(p,n)^{18}F nuclear reaction by bombardment of 98% ^{18}O-enriched [^{18}O]H_2O (Rotem Industries Ltd., Arava, Israel) with 16 MeV protons in a 1.6 mL silver liquid target using a GE PETtrace™ 800 cyclotron (GE Healthcare GmbH, Munich, Germany). Radioactivity was measured with a Curiementor 2 from PTW GmbH (Freiburg, Germany). Labeling reactions were performed in 5 mL V-Vials equipped with a PTFE-coated stirring bar and a silicone septum. Solutions were handled with disposable medical syringes and cannulas. All temperatures refer to the temperature of the metal heating block. Radiochemical yields were determined based on the isolated product activity. The radiochemical purity was determined by analytical HPLC with post-column injection[38] (Fig. S2). The concentration of chemical impurities was determined based on the UV trace, assuming similar weights and absorption coefficients compared to 1-NBX.

Radiosynthesis of [^{18}F]1-NBX ([^{18}F]11a)

A V-Vial was charged with Kryptofix 2.2.2 (9 mg), an aqueous solution of K_2CO_3 (1 M, 12 µL), [^{18}F]fluoride in [^{18}O]water (100 – 200 µL) and acetonitrile (1 mL). The vial was sealed with a septum and heated to 85 °C under reduced pressure (600 mbar) in a stream of argon for 5 min followed by two subsequent additions of anhydrous acetonitrile and evaporation to dryness. The residue was heated to 85 °C at 10 mbar for 3 min and the vial was backflushed with argon. The labelling precursor (5 mg) dissolved in anhydrous DMSO (500 µL) was then added and the mixture was stirred at 85 °C for 10 min. The vial was cooled in a water bath at room temperature for 1 min before the addition of 2 M aqueous NaOH (200 µL). After 3 minutes, the crude product was diluted with water (1 mL) and TFA (60 µL) and subjected to semipreparative HPLC purification (Phenomenex Gemini C18 5µm, 250 x 10 mm, 50% acetonitrile, 0.1% TFA, 4.7 mL/min, λ=270 nm)(Fig. S3). The product fractions had a sufficiently high activity concentration to be directly used for the in vitro experiments.

Determination of logP

2 mL Eppendorf vials were charged with 1-octanol and water (750 µL of each) followed by addition of 1 µL of the tracer solution (50-100 kBq). The vials were vigorously shaken on a vortex mixer for 5 min and then centrifuged at 20000 rcf for 5 min. Approximately 400 µL of the upper 1-octanol phase were carefully removed from the top, while approximately 400 µL of the aqueous phase were removed by piercing the bottom of the vial with a syringe and cannula. Exactly 300 µL of each fraction were then transferred into fresh vials and counted in a gamma counter (HIDEX, Turku, Finland).

4.7. In vitro studies

Autoradiography

Tissue harvesting for autoradiography was conducted in accordance with the EU directive 2010/63/EU for animal experiments and the German Animal Welfare Act (TierSchG, 2006). Male Sprague Dawley rats (body weight 400-500 g) were killed by decapitation and the brains were rapidly removed and immediately frozen by immersion in isopentane (-50 °C). Horizontal slices (20 µm) were cut at -18 °C on a Leica CM3050 cryostat (Leica Biosystems, Nussloch, Germany), thaw-mounted onto silica-coated object slides, dried at 37 °C and stored at -80 °C in vacuum-sealed plastic bags until use. Incubations were conducted in Tris buffer (50 mM Tris-HCl, pH 7.4) at 21 °C. Following a 5 min preincubation step in buffer, the slices were incubated in buffer containing 100 µM guanosine-5'-triphosphate (GTP), 1 mM EDTA and 6 pM [^{18}F]1-NBX for 60 min. Non-specific binding was determined in the presence of the competing ligand [^{3}H]DPCPX (1 µM). Slices were washed twice for 1 min in buffer (5 °C), immersed in ice-cold deionized water, dried at 37 °C and exposed to a phosphor imaging plate. The plate was analyzed with a phosphor imager (BAS 5000, Fujifilm, Düsseldorf, Germany) and tracer binding was quantified via 2D densitometry (AIDA Image Analysis software V5.1). Specific binding was calculated as the difference between total and non-specific binding (4 slices each).

Stable transfection of CHO cells

Human adenosine receptors ADORA1 and ADORA2A from human whole brain cDNA (Clontech) cloned into a pcDNA3.1+ vector (Invitrogen) at EcoRI (5'), XhoI (3') for ADORA1 and BamHI(5'), XhoI (3') for ADORA2A were purchased from The Missouri S&T cDNA Resource Center, USA. Plasmid DNA was amplified and purified using standard molecular biological techniques. For transfection, a modified version of the calcium phosphate precipitation method was used[39]. Briefly, 4×10^5 CHO-K1 cells were seeded in 6 cm Petri dishes and transfected with 8 µg of human A_1R- or A_{2A}R-encoding plasmid DNA for 20 h at 37 °C. Selection of stably transfected cells was initiated with 1 mg/mL geneticin (G418) until cell colonies had formed. From these colonies, single clonal lines were isolated by limiting dilution. Propagation of receptor expressing cells was performed in medium containing 450 µg/mL G418. Expression of human A_1R or A_{2A}R was verified by ligand binding ([^{3}H]DPCPX or [^{3}H]ZM241385) and Western blotting.

Cell culture

Transfected and non-transfected CHO cells were grown adherently under standard growth conditions (37 °C and 5% CO_2) in Ham's F12 Nutrient Mixture supplemented with 10% fetal bovine serum (FBS), penicillin (100 U/mL), streptomycin (100 µg/mL), L-glutamine (2 mM) and geneticin (G418, 0.2 mg/mL). Cells were split two or three times a week at ratios between 1:3 and 1:10. For binding assays, the culture medium was removed, the cells were washed with PBS (pH 7.4), scraped off, suspended in 1 mL PBS per dish and stored at −80 °C. The Caco-2 cell line for the permeability assays was obtained from the Leibniz Institute DSMZ-German Collection of Microorganisms and Cell Cultures GmbH (Braunschweig, Germany) and grown under standard growth conditions (37 °C and 5% CO_2) in Minimum Essential Medium with 2 mM L-alanyl-glutamine (MEM GlutaMAX) supplemented with 10% FBS and 1% antibiotic-antimycotic-mix (Gibco Anti-Anti). Routine cultures were maintained in 9 cm petri dishes and the culture medium was replaced twice a week. Cells were split at about 80% confluency using standard trypsinization techniques.

Preparation of Caco-2 cell monolayers and permeability assays

For the permeability assays, Caco-2 cells were seeded on gelatin-coated 24-well cell culture inserts (PET membrane with 0.4 µm pore size; cellQART, Northeim, Germany) at a density of 50,000 cells/ml. The culture medium (200 µL in the apical and 1200 µL in the basolateral chamber) was carefully replaced twice a week. After a culture period of about 24 – 28 days, the Caco-2 cell monolayers were used for the permeability studies. The transepithelial electrical resistance (TEER) of the monolayers was assessed prior to each exchange of culture medium or prior to each permeability assay, respectively, and only monolayers exhibiting TEER values above 600 Ω × cm^2 were used for the assays. In control experiments, TEER values above 600 Ω × cm^2 correlated with a permeability coefficient of about 5.7 × 10^{-7} cm/s for the paracellular marker fluorescein, which has been shown to be sufficiently low to perform reliable permeation assays[40].

Before the experiments, the culture medium in the apical and basolateral chambers was replaced with Dulbecco´s Phosphate Buffered Saline (DPBS; with Ca/Mg). After an equilibration period of 30 min, the permeability assays were started by replacing 200 µL of the DPBS in the apical compartment with an equal volume of DPBS containing 185 kBq/mL of the respective radiotracer. Control inserts without cells were used to determine the permeability coefficient of the cell-free membrane inserts (P_m). All experiments were performed in an Eppendorf ThermoMixer (Eppendorf Vertrieb Deutschland GmbH, Wesseling-Berzdorf, Germany) at 37 °C and 400 rpm. Samples of 1 mL were taken from the basolateral compartment after 10 min (controls) or 60 min (cell layers) and measured in a gamma counter (HIDEX, Turku, Finland).

Permeability coefficients (P) were calculated according to[41]:

$$P\ [cm/s] = \frac{V_d\ x\ \Delta M_r}{A\ x\ M_d\ x\ \Delta t} \qquad \text{(Eq. 1)}$$

where V_d is the volume in the apical compartment (in cm^3), ΔM_r is the total amount of radiotracer in the basolateral compartment after t seconds, M_d is the total amount of radiotracer added (at time 0) to the apical compartment, Δt is the incubation time (in seconds) and A is the area of the membrane (in cm^2).

The permeability coefficient of the cell layer (P_c) was calculated according to:

$$\frac{1}{P_c} = \frac{1}{P_t} - \frac{1}{P_m} \qquad \text{(Eq. 2)}$$

where P_m is permeability coefficient of the cell-free membrane insert and P_t the total permeability coefficient of the whole system (P_t).

Membrane preparation

Membranes for the ligand binding experiments were prepared using a modified version of an established protocol: Frozen cell samples were thawed and homogenized on ice (Ultra-Turrax, 1 x 30 sec at full speed)[42]. The homogenate was centrifuged at 600 × g for 10 min at 4 °C. To collect the membrane fraction, the supernatant was centrifuged at 50,000 × g for 60 min at 4 °C. The resulting membrane pellet was re-suspended in 50 mM Tris/HCl buffer (pH 7.4), frozen in liquid nitrogen at a protein concentration of 6 mg/mL and stored at -80 °C. Protein content was determined with a naphthol blue black photometric assay after solubilization in 15% NH_4OH containing 2% SDS (w/v) using human serum albumin as a standard[43].

Binding studies

Binding experiments were performed with membranes from CHO-K1 cells stably transfected with either the human A_1 or A_{2A} adenosine receptor prepared as described above. Membrane homogenates with a protein content of 7.5 µg were immobilized in a gel matrix as described earlier[44]. Dissociation constants (K_ds) of the competing radioligands [^{3}H]DPCPX (for A_1R) and [^{3}H]ZM241385 (for A_{2A}R) were determined by saturation binding studies to be 2.9 ± 0.6 nM (n=4) and 1.3 ± 0.4 nM (n=3), respectively. Inhibitory constants (K_is) were determined by competition binding studies. The embedded membrane fragments were incubated with the tritiated radioligands and varying concentrations of the non-radioactive norbonane-substituted xanthine ligands **11a-c** and **17** (A_1R: 0.35 nM [^{3}H]DPCPX + 0.2 nM – 1 µM ligand; A_{2A}R: 0.3 nM [^{3}H]ZM241385, + 0.6 nM – 5 µM ligand) in a total volume of 1.5 mL 50 mM Tris/HCl buffer (pH 7.4). After an incubation time of 70 min, the immobilized membrane homogenates were washed with water and transferred into scintillation cocktail (5 mL each, Ultima Gold, Perkin Elmer). The radioactivity of the samples (bound radioactivity) was measured with a liquid scintillation counter (Beckman, USA). All binding data were calculated by non-linear regression with a computer aided curve fitting program (Prism version 4.0, GraphPad Software, Inc., La Jolla, USA). Binding studies with [^{18}F]1-NBX and [^{18}F]CPFPX were performed under the same conditions as described above using immobilized membrane homogenates from A_1R-transfected CHO-K1 cells or the corresponding (non-

transfected) CHO-K1 wildtype cells, 2.5 kBq/mL of the respective radioligand (8-25 pM) and DPCPX (2 µM) as competing ligand.

Oxidation of xanthines by human liver microsomes

Liver microsomes (0.8 mg protein) were dispersed in 0.1 M phosphate buffer (pH 7.4) containing 3.3 mM $MgCl_2$ and a NADPH-generating system consisting of 1.3 mM NADP, 3.3 mM glucose 6-phosphate and 0.4 U glucose 6-phosphate dehydrogenase in a final volume of 999 µL. After 5 min of preincubation at 37 °C in a shaking incubator, the reactions were initiated by addition of 1 µL 10 mM substrate solutions in DMSO (final concentration 10 µM; 0.1% DMSO).

Rate of microsomal metabolism

The microsomal reactions were initiated by addition of the respective compound following a 5 min preincubation of the other assay components at 37 °C as described above. Aliquots of 75 µL were taken at various time points (10 – 300 minutes) after addition of the respective compound and quenched with 75 µL acetonitrile. After two minutes of vortexing and centrifugation (20.000 × g, 2 min), 100 µL of the supernatants were analyzed by HPLC (Column: Kromasil – 5RP18, 250 × 4,6 mm; eluent: methanol/water/acetic acid, 75:25:0.2, v/v/v; flowrate 1 mL/min; UV-detection at 275 nm). At least three independent experiments were performed per time point.

LC-MS analysis of microsomal metabolites

The microsomal reaction was initiated by addition of 1-NBX following a 5 min preincubation of the other assay components at 37 °C as described above and stopped after 60 min by addition of acetonitrile (2 mL). After 2 min of vortexing and centrifugation (20.000 x g, 4 °C, 1 min), the supernatant was evaporated to dryness under reduced pressure at ambient temperature. The samples were then reconstituted with 100 µL HPLC eluent consisting of acetonitrile/H_2O/acetic acid 35:65:0.1 (v/v/v). After centrifugation for 3 min at 20,000 x g (21 °C), 33 µL of the clear supernatant was injected onto a Kromasil C18 column. The UV-detector outlet was coupled to a mass spectrometer (MSQ PlusTM, Thermo Electron Corporation, San Jose, CA, USA) via an electrospray interface. LC-MS parameters were as follows. Nebulizer gas pressure: 6 bar; desolvation temperature: 500 °C; positive ion mode (ESI+); sprayer voltage: 3000 V; cone voltages: 50 V (unfragmented spectra) or 185 V (fragmented spectra), m/z range 1–800; scan time: 1 s. Mass spectra were analyzed using Xcalibur software (version 3.0).

5. Supplementary data

NMR spectra and HPLC traces of synthesized compounds; additional data for the rate of metabolism in human liver microsomes (PDF).

6. Author contributions

Swen Humpert: Methodology, Validation, Investigation, Writing - Original Draft, Writing - Review & Editing, Visualization **Daniela Schneider**: Methodology, Validation, Investigation, Formal analysis, Writing - Original Draft, Writing - Review & Editing, Visualization **Dirk Bier**: Conceptualization, Methodology, Validation, Investigation, Formal analysis, Writing - Original Draft, Writing - Review & Editing, Visualization **Anette Schulze**: Validation, Investigation **Felix Neumaier**: Writing - Original Draft, Writing - Review & Editing, Visualization **Bernd Neumaier**: Writing - Review & Editing, Funding acquisition, Supervision, Project administration **Marcus Holschbach**: Conceptualization, Methodology, Validation, Investigation, Writing - Original Draft, Visualization, Supervision, Project administration

7. Acknowledgements

This research did not receive any specific grant from funding agencies in the public, commercial, or not-for-profit sectors.

8. Competing interests statement

The authors declare that they have no known competing financial interests or personal relation-ships that could have appeared to influence the work reported in this paper.

9. References

1. Boison, D., Adenosine as a modulator of brain activity. *Drug news & perspectives* **2007,** *20* (10), 607-611.
2. Porkka-Heiskanen, T., Adenosine in sleep and wakefulness. *Annals of medicine* **1999,** *31* (2), 125-129.
3. De Mendonça, A.; Ribeiro, J. A., Adenosine and synaptic plasticity. *Drug development research* **2001,** *52* (1-2), 283-290.
4. Rahman, A., The role of adenosine in Alzheimer's disease. *Current neuropharmacology* **2009,** *7* (3), 207-216.
5. (a) Morelli, M.; Carta, A.; Jenner, P., Adenosine receptors in health and disease. *Handb Exp. Pharmacol* **2009,** *193*, 589-615; (b) Morelli, M.; Carta, A. R.; Jenner, P., Adenosine A 2A receptors and Parkinson's disease. *Adenosine receptors in health and disease* **2009**, 589-615.
6. Sebastiao, A. M.; Ribeiro, J. A., Adenosine receptors and the central nervous system. *Adenosine receptors in health and disease* **2009**, 471-534.
7. (a) Paul, S.; H Elsinga, P.; Ishiwata, K.; AJO Dierckx, R.; Van Waarde, A., Adenosine A1 receptors in the central nervous system: their functions in health and disease, and possible elucidation by PET imaging. *Current medicinal chemistry* **2011,** *18* (31), 4820-4835; (b) Mishina, M.; Ishiwata, K., Adenosine receptor PET imaging in human brain. *International review of neurobiology* **2014,** *119*, 51-69.
8. Holschbach, M. H.; Olsson, R. A.; Bier, D.; Wutz, W.; Sihver, W.; Schüller, M.; Palm, B.; Coenen, H. H., Synthesis and evaluation of no-carrier-added 8-cyclopentyl-3-(3-[18F] fluoropropyl)-1-propylxanthine ([18F] CPFPX): a potent and selective A1-adenosine receptor antagonist for in vivo imaging. *Journal of medicinal chemistry* **2002,** *45* (23), 5150-5156.
9. (a) Nabbi-Schroeter, D.; Elmenhorst, D.; Oskamp, A.; Laskowski, S.; Bauer, A.; Kroll, T., Effects of long-term caffeine consumption on the adenosine A 1 receptor in the rat brain: An in vivo PET

study with [18 F] CPFPX. *Molecular Imaging and Biology* **2018,** *20*, 284-291; (b) Meyer, P. T.; Elmenhorst, D.; Boy, C.; Winz, O.; Matusch, A.; Zilles, K.; Bauer, A., Effect of aging on cerebral A1 adenosine receptors: a [18F] CPFPX PET study in humans. *Neurobiology of aging* **2007,** *28* (12), 1914-1924; (c) Elmenhorst, D.; Elmenhorst, E.-M.; Hennecke, E.; Kroll, T.; Matusch, A.; Aeschbach, D.; Bauer, A., Recovery sleep after extended wakefulness restores elevated A1 adenosine receptor availability in the human brain. *Proceedings of the National Academy of Sciences* **2017,** *114* (16), 4243-4248; (d) Matusch, A.; Saft, C.; Elmenhorst, D.; Kraus, P. H.; Gold, R.; Hartung, H.-P.; Bauer, A., Cross sectional PET study of cerebral adenosine A 1 receptors in premanifest and manifest Huntington's disease. *European journal of nuclear medicine and molecular imaging* **2014,** *41*, 1210-1220.

10. Schneider, D.; Oskamp, A.; Holschbach, M.; Neumaier, B.; Bauer, A.; Bier, D., Relevance of in vitro metabolism models to PET radiotracer development: prediction of in vivo clearance in rats from microsomal stability data. *Pharmaceuticals* **2019,** *12* (2), 57.

11. Holschbach, M. H.; Bier, D.; Sihver, W.; Schulze, A.; Neumaier, B., Synthesis and Pharmacological Evaluation of Identified and Putative Metabolites of the A1 Adenosine Receptor Antagonist 8-Cyclopentyl-3-(3-fluoropropyl)-1-propylxanthine (CPFPX). *ChemMedChem* **2017,** *12* (10), 770-784.

12. (a) Bier, D.; Holschbach, M. H.; Wutz, W.; Olsson, R. A.; Coenen, H. H., Metabolism of the A1 adenosine receptor positron emission tomography ligand [18F] 8-cyclopentyl-3-(3-fluoropropyl)-1-propylxanthine ([18F] CPFPX) in rodents and humans. *Drug metabolism and disposition* **2006,** *34* (4), 570-576; (b) Matusch, A.; Meyer, P. T.; Bier, D.; Holschbach, M. H.; Woitalla, D.; Elmenhorst, D.; Winz, O. H.; Zilles, K.; Bauer, A., Metabolism of the A1 adenosine receptor PET ligand [18F] CPFPX by CYP1A2: implications for bolus/infusion PET studies. *Nuclear medicine and biology* **2006,** *33* (7), 891-898.

13. Schneider, D.; Oskamp, A.; Holschbach, M.; Neumaier, B.; Bier, D.; Bauer, A., Influence of binding affinity and blood plasma level on cerebral pharmacokinetics and PET imaging characteristics of two novel xanthine PET radioligands for the A1 adenosine receptor. *Nuclear medicine and biology* **2020,** *82*, 1-8.

14. (a) Bruns, R. F.; Daly, J. W.; Snyder, S. H., Adenosine receptor binding: structure-activity analysis generates extremely potent xanthine antagonists. *Proceedings of the National Academy of Sciences* **1983,** *80* (7), 2077-2080; (b) Smellie, F.; Daly, J.; Wells, J., 1-Isoamyl-3-isobutylxanthine: a remarkably potent agent for the potentiation of norepinephrine, histamine, and adenosine-elicited accumulations of cyclic AMP in brain slices. *Life Sciences* **1979,** *25* (22), 1917-1924; (c) Shimada, J.; Suzuki, F.; Nonaka, H.; Ishii, A., 8-Polycycloalkyl-1, 3-dipropylxanthines as potent and selective antagonists for A1-adenosine receptors. *Journal of medicinal chemistry* **1992,** *35* (5), 924-930.

15. (a) Daly, J. W.; Padgett, W.; Shamim, M.; Butts-Lamb, P.; Waters, J., 1, 3-Dialkyl-8-(p-sulfophenyl) xanthines: potent water-soluble antagonists for A1-and A2-adenosine receptors. *Journal of medicinal chemistry* **1985,** *28* (4), 487-492; (b) Daly, J.; Padgett, W.; Shamim, M., Analogs of 1, 3-dipropyl-8-phenylxanthine: enhancement of selectivity at A1-adenosine receptors by aryl substituents. *Journal of medicinal chemistry* **1986,** *29* (8), 1520-1524.

16. Shamim, M.; Ukena, D.; Padgett, W.; Hong, O.; Daly, J., 8-Aryl-and 8-cycloalkyl-1, 3-dipropylxanthines: further potent and selective antagonists for A1-adenosine receptors. *Journal of medicinal chemistry* **1988,** *31* (3), 613-617.

17. (a) Shimada, J.; Suzuki, F.; Nonaka, H.; Karasawa, A.; Mizumoto, H.; Ohno, T.; Kubo, K.; Ishii, A., 8-(Dicyclopropylmethyl)-1, 3-dipropylxanthine: a potent and selective adenosine A1 antagonist with renal protective and diuretic activities. *Journal of medicinal chemistry* **1991,** *34* (1), 466-469; (b) Peet, N. P.; Lentz, N. L.; Dudley, M. W.; Ogden, A. M. L.; McCarty, D. R.; Racke, M. M., Xanthines with C8 chiral substituents as potent and selective adenosine A1 antagonists. *Journal of medicinal chemistry* **1993,** *36* (25), 4015-4020; (c) Pfister, J. R.; Belardinelli, L.; Lee, G.; Lum, R. T.; Milner, P.; Stanley, W. C.; Linden, J.; Baker, S. P.; Schreiner, G., Synthesis and biological evaluation of the enantiomers of the potent and selective A1-adenosine antagonist 1, 3-dipropyl-8-[2-(5, 6-epoxynorbonyl)]-xanthine. *Journal of medicinal chemistry* **1997,** *40* (12), 1773-1778; (d) Kiesman, W. F.; Zhao, J.; Conlon, P. R.; Dowling, J. E.; Petter, R. C.; Lutterodt, F.; Jin, X.; Smits, G.; Fure, M.; Jayaraj,

A., Potent and orally bioavailable 8-bicyclo [2.2. 2] octylxanthines as adenosine A1 receptor antagonists. *Journal of medicinal chemistry* **2006,** *49* (24), 7119-7131.
18. Castagnino, E.; Salvatori, A.; Corsano, S.; Tacchi, P.; Martini, C.; Lucacchini, A., Effects of substituent size upon adenosine receptor A1/A2 affinity of some newly synthesised 8-cycloalkyl xanthines. *Drug design and discovery* **1995,** *12* (4), 313-321.
19. Boehme, W. R., Stereochemistry of Diels-Alder Adducts. III. The Preparation and Rearrangement of Some Brominated Derivatives of Norbornanecarboxylic Acids. *Journal of the American Chemical Society* **1959,** *81* (11), 2762-2765.
20. Werstiuk, N. H., The Determination of the Preferred Stereochemistry and the Magnitude of the Hydrogen Isotope Effect for 1, 3 Elimination in the Locked Norbornyl System Methyl exo-2-Bromo-1-norbornanecarboxylate-endo, endo-5, 6-d 2. *Canadian Journal of Chemistry* **1975,** *53* (1), 26-40.
21. Gomez R., D. J., Oballa R. M., Powell D. A, Carbocyclic prolinamide derivatives. WO2017/222914, 2017.
22. Stapersma, J.; Klumpp, G., 7-Lithio-norbornadiene. *Tetrahedron* **1981,** *37* (1), 187-189.
23. Freeman, P. K.; Hutchinson, L. L., Organolithium reagents from alkyl halides and lithium DI-tert-butylbiphenyl. *Tetrahedron Letters* **1976,** *17* (22), 1849-1852.
24. Holschbach, M. H.; Bier, D.; Wutz, W.; Willbold, S.; Olsson, R. A., Synthesis of the main metabolite in human blood of the A1 adenosine receptor ligand [18F] CPFPX. *Organic letters* **2009,** *11* (19), 4266-4269.
25. Yoshida, Y.; Shimonishi, K.; Sakakura, Y.; Okada, S.; Aso, N.; Tanabe, Y., Facile and practical methods for the sulfonylation of alcohols using Ts (Ms) Cl and Me2N (CH2) nNMe2 as a key base. *Synthesis* **1999,** *1999* (09), 1633-1636.
26. Kim, D. W.; Ahn, D.-S.; Oh, Y.-H.; Lee, S.; Kil, H. S.; Oh, S. J.; Lee, S. J.; Kim, J. S.; Ryu, J. S.; Moon, D. H., A new class of SN2 reactions catalyzed by protic solvents: facile fluorination for isotopic labeling of diagnostic molecules. *Journal of the American Chemical Society* **2006,** *128* (50), 16394-16397.
27. (a) Coenen, H. H.; Schüller, M.; Stöcklin, G.; Klatte, B.; Knöchel, A., Preparation of nca [17-18F]-fluoroheptadecanoic acid in high yields via aminopolyether supported, nucleophilic fluorination. *Journal of Labelled Compounds and Radiopharmaceuticals* **1986,** *23* (5), 455-466; (b) Hamacher, K.; Coenen, H. H.; Stöcklin, G., Efficient stereospecific synthesis of no-carrier-added 2-[18F]-fluoro-2-deoxy-D-glucose using aminopolyether supported nucleophilic substitution. *Journal of nuclear medicine* **1986,** *27* (2), 235-238.
28. (a) Dragojlovic, V., Conformational analysis of cycloalkanes. *ChemTexts* **2015,** *1* (3), 14; (b) Trivedi, B.; Bridges, A.; Patt, W.; Priebe, S.; Bruns, R., N6-Bicycloalkyladenosines with unusually high potency and selectivity for the adenosine A1 receptor. *Journal of medicinal chemistry* **1989,** *32* (1), 8-11.
29. Waterhouse, R. N., Determination of lipophilicity and its use as a predictor of blood–brain barrier penetration of molecular imaging agents. *Molecular Imaging & Biology* **2003,** *5* (6), 376-389.
30. Hellinger, É.; Veszelka, S.; Tóth, A. E.; Walter, F.; Kittel, Á.; Bakk, M. L.; Tihanyi, K.; Háda, V.; Nakagawa, S.; Duy, T. D. H., Comparison of brain capillary endothelial cell-based and epithelial (MDCK-MDR1, Caco-2, and VB-Caco-2) cell-based surrogate blood–brain barrier penetration models. *European journal of pharmaceutics and biopharmaceutics* **2012,** *82* (2), 340-351.
31. Zhang, L.; Villalobos, A., Strategies to facilitate the discovery of novel CNS PET ligands. *EJNMMI Radiopharmacy and Chemistry* **2017,** *1*, 1-12.
32. Fastbom, J.; Pazos, A.; Palacios, J., The distribution of adenosine A1 receptors and 5'-nucleotidase in the brain of some commonly used experimental animals. *Neuroscience* **1987,** *22* (3), 813-826.
33. (a) Bauer, A.; Holschbach, M. H.; Cremer, M.; Weber, S.; Boy, C.; Shah, N. J.; Olsson, R. A.; Halling, H.; Coenen, H. H.; Zilles, K., Evaluation of 18F-CPFPX, a novel adenosine A1 receptor ligand: in vitro autoradiography and high-resolution small animal PET. *Journal of Nuclear Medicine* **2003,** *44* (10), 1682-1689; (b) Elmenhorst, D.; Kroll, T.; Wedekind, F.; Weisshaupt, A.; Beer, S.; Bauer, A., In vivo kinetic and steady-state quantification of 18F-CPFPX binding to rat cerebral A1 adenosine receptors:

validation by displacement and autoradiographic experiments. *Journal of nuclear medicine* **2013,** *54* (8), 1411-1419.
34. (a) Bier, D.; Hartmann, R.; Holschbach, M., Collision-induced dissociation studies of caffeine in positive electrospray ionisation mass spectrometry using six deuterated isotopomers and one N1-ethylated homologue. *Rapid communications in mass spectrometry* **2013,** *27* (8), 885-895; (b) Schneider, D.; Bier, D.; Holschbach, M.; Bauer, A.; Neumaier, B., Species differences in microsomal metabolism of xanthine-derived A1 adenosine receptor ligands. *Pharmaceuticals* **2021,** *14* (3), 277.
35. Fredholm, B. B.; Arnaud, M. J., Pharmacokinetics and metabolism of natural methylxanthines in animal and man. *Methylxanthines* **2011**, 33-91.
36. Armarego, W. L., *Purification of laboratory chemicals*. Butterworth-Heinemann: 2017.
37. Kelly M.G., C. W. E., Harrison B.L., Zhang G., Bravo B.A., Schechter L.E. Preparation of bicyclic indolyl piperazine derivatives as serotonergic agents. WO2004/111035, 2004, A1.
38. Humpert, S.; Hoffmann, C.; Neumaier, F.; Zlatopolskiy, B. D.; Neumaier, B., Validation of analytical HPLC with post-column injection as a method for rapid and precise quantification of radiochemical yields. *Journal of Chromatography B* **2023,** *1228*, 123847.
39. (a) Wachten, S.; Schlenstedt, J.; Gauss, R.; Baumann, A., Molecular identification and functional characterization of an adenylyl cyclase from the honeybee. *Journal of neurochemistry* **2006,** *96* (6), 1580-1590; (b) Chen, C.; Okayama, H., High-efficiency transformation of mammalian cells by plasmid DNA. *Molecular and cellular biology* **1987,** *7* (8), 2745-2752.
40. (a) Berginc, K.; Žakelj, S.; Levstik, L.; Uršič, D.; Kristl, A., Fluorescein transport properties across artificial lipid membranes, Caco-2 cell monolayers and rat jejunum. *European journal of pharmaceutics and biopharmaceutics* **2007,** *66* (2), 281-285; (b) Koljonen, M.; Hakala, K. S.; Ahtola-Sätilä, T.; Laitinen, L.; Kostiainen, R.; Kotiaho, T.; Kaukonen, A. M.; Hirvonen, J., Evaluation of cocktail approach to standardise Caco-2 permeability experiments. *European journal of pharmaceutics and biopharmaceutics* **2006,** *64* (3), 379-387.
41. Di Marco, A.; Gonzalez Paz, O.; Fini, I.; Vignone, D.; Cellucci, A.; Battista, M. R.; Auciello, G.; Orsatti, L.; Zini, M.; Monteagudo, E., Application of an in vitro blood–brain barrier model in the selection of experimental drug candidates for the treatment of Huntington's disease. *Molecular Pharmaceutics* **2019,** *16* (5), 2069-2082.
42. Lohse, M. J.; Lenschow, V.; Schwabe, U., Interaction of barbiturates with adenosine receptors in rat brain. *Naunyn-Schmiedeberg's archives of pharmacology* **1984,** *326*, 69-74.
43. NEUHOFF, V.; PHILIPP, K.; ZIMMER, H.-G.; Mesecke, S., A simple, versatile, sensitive and volume-independent method for quantitative protein determination which is independent of other external influences. **1979**.
44. Bier, D.; Schulze, A.; Holschbach, M.; Neumaier, B.; Baumann, A., Development and evaluation of a versatile receptor-ligand binding assay using cell membrane preparations embedded in an agarose gel matrix and evaluation with the human adenosine A1 receptor. *Assay and drug development technologies* **2020,** *18* (7), 328-340.